Precision modeling of breast cancer in the CRISPR era

Annunziato, S.

3

Modeling invasive lobular breast carcinoma by CRISPR/Cas9-mediated somatic genome editing of the mammary gland

Stefano Annunziato[a*], Sjors M. Kas[a*], Micha Nethe[a], Hatice Yücel[a], Jessica Del Bravo[b], Colin Pritchard[b], Rahmen Bin Ali[b], Bas van Gerwen[c], Bjørn Siteur[c], Anne Paulien Drenth[a], Eva Schut[a], Marieke van de Ven[c], Mirjam C. Boelens[a], Sjoerd Klarenbeek[d], Ivo J. Huijbers[b], Martine H. van Miltenburg[a] and Jos Jonkers[a,e]

[a] Division of Molecular Pathology, The Netherlands Cancer Institute, Plesmanlaan 121, 1066 CX Amsterdam, The Netherlands
[b] Mouse Clinic for Cancer and Aging (MCCA) Transgenic Core Facility, The Netherlands Cancer Institute, Plesmanlaan 121, 1066 CX Amsterdam, The Netherlands
[c] Mouse Clinic for Cancer and Aging (MCCA) Preclinical Intervention Unit, The Netherlands Cancer Institute, Plesmanlaan 121, 1066 CX Amsterdam, The Netherlands
[d] Experimental Animal Pathology, The Netherlands Cancer Institute, Plesmanlaan 121, 1066 CX Amsterdam, The Netherlands
[e] Cancer Genomics Netherlands, The Netherlands Cancer Institute, Plesmanlaan 121, 1066 CX Amsterdam, The Netherlands
* The first two authors contributed equally to this work

Published in *Genes & Development*, 2016 Jun 15.

Abstract

Large-scale sequencing studies are rapidly identifying putative oncogenic mutations in human tumors. However, the discrimination between passenger and driver events in tumorigenesis remains challenging and requires *in vivo* validation studies in reliable animal models of human cancer. In this study we describe a novel strategy for *in vivo* validation of candidate tumor suppressors implicated in invasive lobular breast carcinoma (ILC), which is hallmarked by loss of the cell-cell adhesion molecule E-cadherin. We describe an approach to model ILC by intraductal injection of lentiviral vectors encoding Cre recombinase, the CRISPR/Cas9 system or both in female mice carrying conditional alleles of the *Cdh1* gene, encoding for E-cadherin. Using this approach we were able to target ILC-initiating cells and to induce specific gene disruption of *Pten* by CRISPR/Cas9-mediated somatic gene editing. Whereas intraductal injection of Cas9-encoding lentiviruses induced Cas9-specific immune responses and development of tumors that did not resemble ILC, lentiviral delivery of a *Pten*-targeting sgRNA in mice with mammary gland-specific loss of E-cadherin and expression of Cas9 efficiently induced ILC development. This versatile platform can be used for rapid *in vivo* testing of putative tumor suppressor genes implicated in ILC, providing new opportunities for modeling invasive lobular breast carcinoma in mice.

Introduction

Invasive lobular carcinoma (ILC) is the second most common type of human breast cancer, accounting for 8-14% of all breast cancer cases (Martinez *et al.*, 1979; Borst *et al.*, 1993; Wong *et al.*, 2014). It is characterized by discohesive epithelial cells infiltrating the surrounding tissue in single-file patterns, accompanied by an abundant presence of fibroblasts and collagen deposition. The majority of human ILCs show loss of the cell-cell adhesion protein E-cadherin due to inactivating mutations, loss-of-heterozygosity (LOH) and methylation of the *CDH1* gene promoter (Moll *et al.*, 1993; Vos *et al.*, 1997; Droufakou *et al.*, 2001; Ciriello *et al.*, 2015) or impaired integrity of the E-cadherin-catenin membrane complex (Rakha *et al.*, 2010). Intriguingly, mice with tissue-specific loss of E-cadherin in mammary epithelial cells do not develop mammary tumors (Boussadia *et al.*, 2002; Derksen *et al.*, 2006; Derksen *et al.*, 2011). It has been shown that E-cadherin loss in mammary epithelial cells leads to apoptosis (Boussadia *et al.*, 2002). However, multifocal ILC development is induced by combined (mammary) epithelium-specific loss of E-cadherin and p53 (Derksen *et al.*, 2006; Derksen *et al.*, 2011) or E-cadherin and PTEN (Boelens *et al.*, 2016), highlighting the importance of co-occurring mutations in ILC development.

Recent studies have shed light on the mutational landscape of human ILC, showing that *CDH1* mutations are accompanied by alterations in a plethora of additional genes, of which only few have been mechanistically linked to ILC formation or tumorigenesis in general (Ciriello *et al.*, 2015). Discrimination between passenger mutations and *bona fide* driver events has become an urgent priority that requires well-designed validation studies in model systems. A gene-by-gene approach can have several bottlenecks, especially when *in vivo* mouse models with complex genotypes have to be generated. Forward genetic approaches in E-cadherin-deficient mouse models can help disentangling this complexity, but promising “hits” from screens ultimately need *ad hoc* validation experiments.

For these reasons, new technologies are needed to expand the genetic toolbox of cancer biologists and to allow a more rapid and systematic *in vivo* interrogation of gene perturbations. In this regard, the advent of CRISPR/Cas9 technologies for somatic genome editing has already paved the way for a new generation of non-germline animal tumor models. For example, liver-specific gene disruption was achieved by transient delivery of components of the CRISPR/Cas9 system in the tail vein of mice, leading to hepatocellular carcinoma (Xue *et al.*, 2014; Weber *et al.*, 2015). Similar approaches have been used to deliver targeted oncogenic mutations to the lung (Platt *et al.*, 2014; Sánchez-Rivera *et al.*, 2014), brain (Zuckermann *et al.*, 2015) and pancreas (Chiou *et al.*, 2015).

Here we describe a novel approach to model ILC by delivering lentiviral vectors to the adult mammary gland by intraductal injection. We show that administration of Cre-encoding lentiviruses results in sporadic targeting of mammary epithelial cells and initiation of multifocal tumor development in mice harboring, together with conditional *Cdh1* alleles, a conditional activating *Akt-E17K* mutation or conditional *Pten* alleles. Furthermore, we implemented CRISPR/Cas9-mediated somatic gene editing in mammary tissue, and as a proof of concept, inactivated PTEN expression in E-cadherin-deficient mammary epithelial cells. However, somatic delivery of Cas9 resulted in mammary tumors that did not resemble ILC and showed strong immune infiltrate, which is most likely due to previously reported Cas9-specific immune responses (Wang *et al.*, 2015). In contrast, intraductal injection of lentiviruses encoding a single-guide RNA (sgRNA) targeting *Pten* in female mice with mammary-specific loss of E-cadherin and expression of Cas9 endonuclease from a conditional knock-in allele resulted in ILC formation without a massive influx of immune cells. Collectively, we describe a platform that can be used for rapid *in vivo* validation of candidate tumor suppressors implicated in ILC, and for development of novel mouse models of this breast cancer subtype.

Results

Transduction of ductal epithelial cells by intraductal injection of lentiviral Cre

Site-specific delivery of adenoviral or lentiviral Cre has been successfully employed in several conditional mouse models to initiate tumor formation in different tissues including lung, liver, muscle and pancreas (Meuwissen *et al.*, 2001; Harada *et al.*, 2004; Kirsch *et al.*, 2007; Chiou *et al.*, 2015). In our study we set out to implement intraductal injections of lentiviral vectors as a tool to achieve mammary gland-specific Cre expression and/or CRISPR/Cas9-mediated genome editing. In the past, intraductal injection of Cre-encoding adenoviruses was successfully used to activate expression of oncogenic fusion genes in the mammary gland of genetically engineered mice leading to mammary tumors (Tao *et al.*, 2014; Rutkowski *et al.*, 2014). To verify the applicability of this technique for intraductal delivery of lentiviruses we performed injections of female virgin FVB mice with a lentiviral vector expressing GFP (n=8), revealing efficient transduction of the ductal tree (Figure 1A, Supplementary Figure S1A-B). To confirm that lentiviral delivery of Cre was capable to recombine conditional alleles *in vivo*, we performed injection of a Cre-encoding lentiviral vector (Lenti-Cre) into double-fluorescent *mT/mG* Cre-reporter mice (n=8), in which membrane-targeted GFP (mGFP) is expressed after Cre-mediated excision of mTomato (Muzumdar *et al.*, 2007). GFP-positive cells were observed throughout the ductal trees of mammary glands from *mT/mG* mice injected with Lenti-Cre (Figure 1B). Immunostaining of mammary gland sections with an anti-GFP antibody showed extensive GFP labeling both in luminal and basal cells of the ductal epithelium at 2 weeks post-injection (Figure 1C-D). Similar results were observed with intraductal injection of Adeno-Cre in *mT/mG* mice (Supplementary Figure S1C-D). These data demonstrate that intraductal injection of Cre-encoding lentiviruses induces efficient *in vivo* recombination of conditional alleles in mammary epithelium, as previously shown by other groups using Adeno-Cre (Russell *et al.*, 2003; Tao *et al.*, 2014; Rutkowski *et al.*, 2014).

Intraductal injection of Lenti-Cre promotes ILC formation in mice carrying conditional alleles of ILC drivers

Next, we investigated whether intraductal injections could be used to initiate mammary tumor formation in genetically engineered mice carrying conditional alleles of genes implicated in human ILC. For this purpose we developed a genetically engineered mouse model in which transgenic Cre expression under transcriptional control of the *Wap* gene promoter induces mammary gland-specific inactivation of E-cadherin and activation of the oncogenic AKT-E17K isoform. These mice were generated by introduction of a Cre-conditional *invCAG-AktE17K-IRES-Luc* allele into the *Col1a1* locus

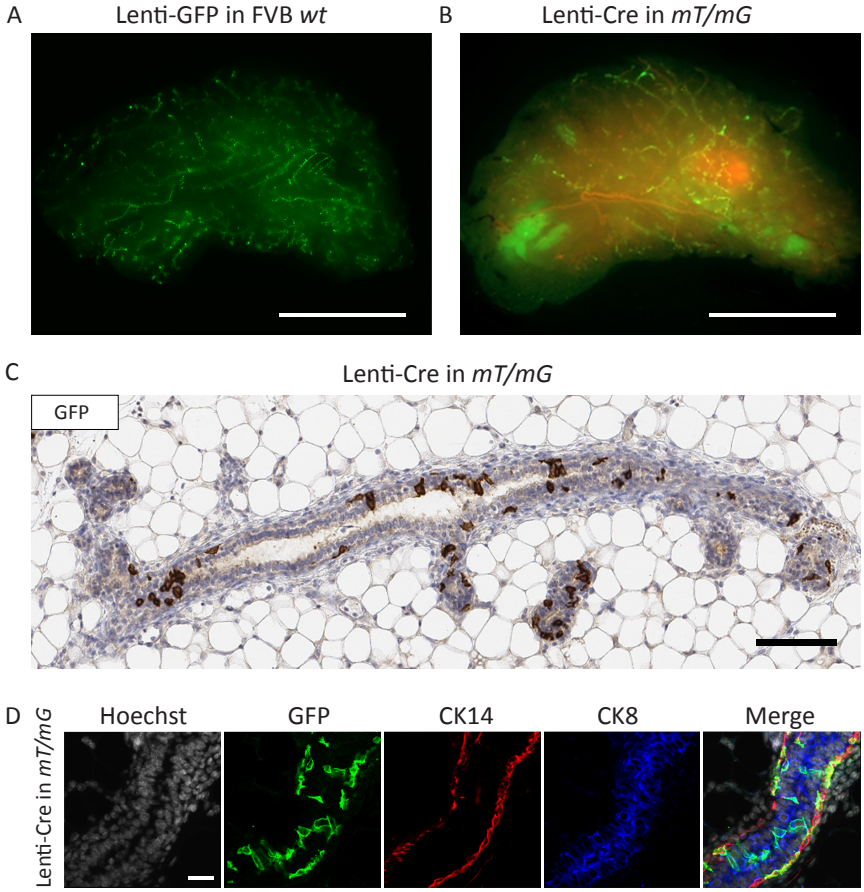

Figure 1 Intraductal injection of Lenti-Cre allows *in vivo* recombination in the mammary epithelium. (A) Fluorescence microscopy of GFP expression in a representative whole mount mammary gland after intraductal injection of Lenti-GFP in FVB wild-type animals (n=8). Mice were analyzed 14 days after injection. Bar = 5 mm. (B) Fluorescence microscopy of GFP expression in a representative whole mount mammary gland after intraductal injection of Lenti-Cre in *mT/mG* Cre-reporter mice (n=8). Mice were analyzed 14 days after injection. Bar = 5 mm. (C) Immunohistochemical detection of GFP expression in a representative mammary gland section from *mT/mG* Cre-reporter mice intraductally injected with Lenti-Cre. Bar = 100 µm. (D) Immunofluorescence analysis of mammary gland sections from Lenti-Cre injected *mT/mG* Cre-reporter mice, showing GFP expression in CK8 and CK14 positive cells. Bar = 25 µm.

of embryonic stem cells (ESCs) derived from *WapCre;Cdh1$^{F/F}$* mice and subsequent production of chimeric mice by blastocyst injection of the modified ESCs (Huijbers *et al.*, 2014; Supplementary Figure S2A-B). High-quality male chimeras were mated with *Cdh1$^{F/F}$* females to generate a cohort of *WapCre;Cdh1$^{F/F}$;Col1a1$^{invCAG\text{-}AktE17K\text{-}IRES\text{-}Luc/+}$* (*WapCre;Cdh1$^{F/F}$;Akt-E17K*) female mice (n=15), which were monitored for spontaneous tumor development. In parallel, *WapCre*-negative *Cdh1$^{F/F}$;Col1a1$^{invCAG\text{-}AktE17K\text{-}IRES\text{-}Luc/+}$* (*Cdh1$^{F/F}$;Akt-E17K*) female mice (n=7) were used for intraductal injections with Lenti-Cre (Figure 2A). All *WapCre;Cdh1$^{F/F}$;Akt-E17K* female mice developed multifocal ILC lesions in all mammary glands due to concomitant inactivation of E-cadherin and expression of the oncogenic AKT-E17K variant accompanied by luciferase expression (Figure 2B). Likewise, intraductal injection of Lenti-Cre into female *Cdh1$^{F/F}$;Akt-E17K* mice resulted in specific bioluminescence signals building up over time (Figure 2C, Supplementary Figure S3A). Following sacrifice of the mice around 30 weeks post-injection (apart for one mouse, which was sacrificed at 12 weeks with a palpable tumor), sectioning and hematoxylin and eosin (H&E) staining of the injected mammary glands revealed multiple tumors in 6 out of 7 injected glands (Supplementary Figure S3B-C). Tumors showed a typical ILC histology with abundant collagen deposition and single files of cytokeratin 8 (CK8) positive tumor cells infiltrating the surrounding tissue. Moreover, tumors showed recombined *Cdh1^{F}* and *invCAG-AktE17K-IRES-Luc* alleles (Supplementary Figure S3D), were phospho-AKT^{Ser473} positive and E-cadherin deficient, and were indistinguishable from those developing in the conventional *WapCre;Cdh1$^{F/F}$;Akt-E17K* model (Figure 2D-E). To investigate if local Lenti-Cre delivery could induce ILC formation driven by loss of tumor suppressor genes (TSGs) rather than activation of a potent oncogene such as *Akt-E17K*, we performed intraductal Lenti-Cre injections in *Cdh1$^{F/F}$;Pten$^{F/F}$* mice (n=8), carrying conditional alleles of E-cadherin and the phosphatase and tensin homologue (*Pten*) gene, a negative regulator of the PI3K/AKT signaling pathway. Again, we observed multifocal ILC formation in 7 out of 8 injected mammary glands following sacrifice of the animals at 14 weeks post-injection. Tumors showed ILC histology, CK8 positive cells and recombined *Cdh1^{F}* and *Pten^{F}* alleles resulting in loss of E-cadherin and PTEN (Figure 2F, Supplementary Figure S4A-D), similar to mammary tumors developing in the *WapCre;Cdh1$^{F/F}$;Pten$^{F/F}$* mouse model (Boelens *et al.*, 2016). Mice injected with control lentiviruses (Lenti-GFP) did not show any ILC formation. Altogether, these data show that intraductal injection of Lenti-Cre in mice carrying conditional alleles of ILC driver genes targets mammary epithelial cells with ILC-initiating capacity, resulting in tumors that closely resemble their human counterparts.

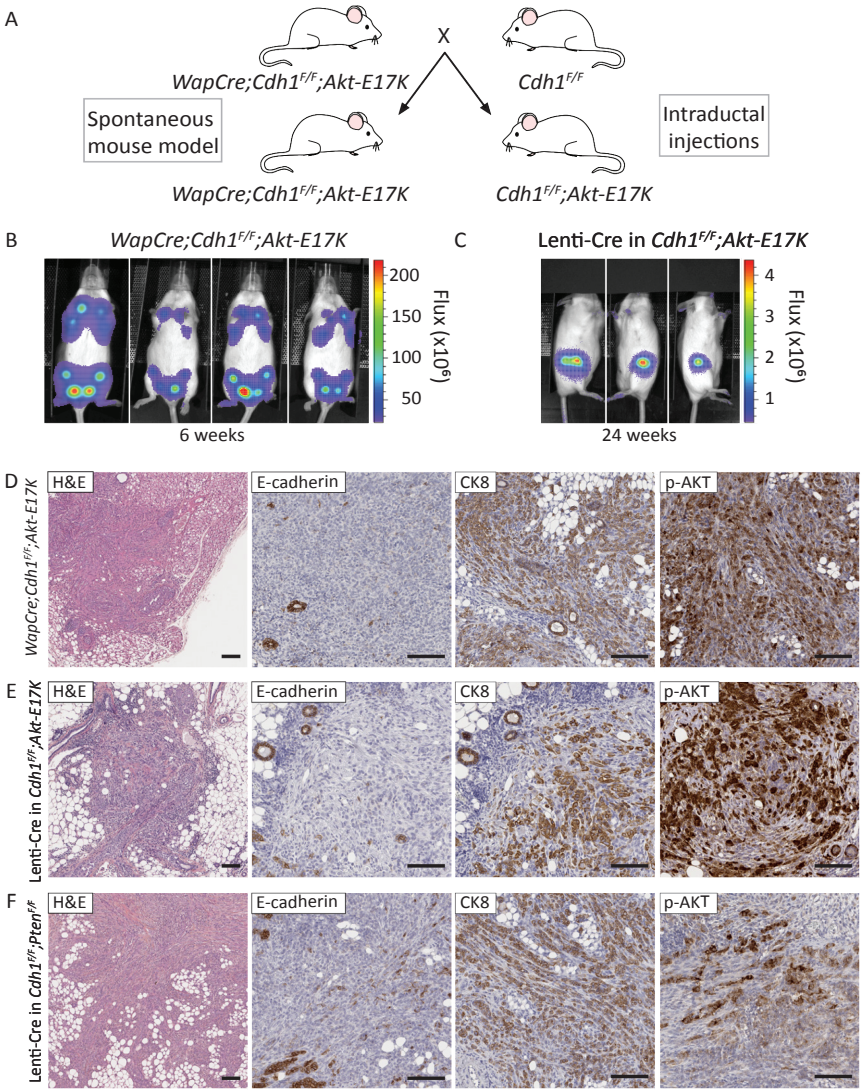

Figure 2 Intraductal injection of Lenti-Cre in *Cdh1*$^{F/F}$*;Akt-E17K* and *Cdh1*$^{F/F}$*;Pten*$^{F/F}$ mice results in ILC formation. (A) Breeding strategy for matched comparison of ILC formation induced by transgenic *WapCre* expression or Lenti-Cre injection in *Cdh1*$^{F/F}$*;Akt-E17K* mice. (B) *In vivo* bioluminescence imaging of luciferase expression in *WapCre;Cdh1*$^{F/F}$*;Akt-E17K* animals at 6 weeks of age. (C) *In vivo* bioluminescence imaging of luciferase expression in *Cdh1*$^{F/F}$*;Akt-E17K* mice 24 weeks after intraductal injection of Lenti-Cre. (D) Immunohistochemical analysis of E-cadherin, CK8 and phospho-AKT^{Ser473} expression in *WapCre;Cdh1*$^{F/F}$*;Akt-E17K* (n=15) tumors. Tumors were analyzed at 6 weeks of age. Bars = 100 µm. (E) Immunohistochemical analysis of E-cadherin, CK8 and phospho-AKT^{Ser473} in tumor sections from Lenti-Cre injected *Cdh1*$^{F/F}$*;Akt-E17K* animals (n=7). Tumor was analyzed 12 weeks after injection. Bars = 100 µm. (F) Immunohistochemistry of E-cadherin, CK8 and phospho-AKT^{Ser473} in tumor sections from Lenti-Cre injected *Cdh1*$^{F/F}$*;Pten*$^{F/F}$ animals (n=8). Tumors were analyzed 14 weeks after injection. Bars = 100 µm.

Intraductal injection of pSECC-sgPten in Cdh1$^{F/F}$ mice induces tumors that do not resemble ILC

Having shown that ILC formation can be induced by intraductal injection of Lenti-Cre in *Cdh1$^{F/F}$;Akt-E17K* and *Cdh1$^{F/F}$;Pten$^{F/F}$* mice, we next explored the possibility of combining local Cre delivery with somatic gene editing by the CRISPR/Cas9 system to rapidly evaluate the contribution of candidate tumor suppressors to ILC formation in *Cdh1$^{F/F}$* mice. For this approach we used the pSECC vector, a lentiviral vector encoding Cre and the CRISPR components (a sgRNA targeting a gene of interest and the *S. pyogenes* Cas9) (Sánchez-Rivera *et al.*, 2014). pSECC vectors containing a non-targeting sgRNA (sgNT) or a validated sgRNA (sg*Pten*) targeting the first exon of *Pten* were tested for their *in vitro* activity in a Cre-reporter cell line carrying a lox-stop-lox GFP cassette. GFP expression and *Pten* gene editing could be achieved efficiently and rapidly upon transduction of GFP-reporter cells with the pSECC-sg*Pten* vector (Figure 3A, Supplementary Figure S5A-B). To assess the *in vivo* recombination efficiency of these lentiviral vectors, we intraductally injected high-titer pSECC-sgNT into *mT/mG* Cre-reporter mice (n=8). GFP staining of mammary glands at 2 weeks post-injection confirmed GFP labeling of ductal epithelial cells (Supplementary Figure S5C). Upon injection of pSECC-sgNT into *Cdh1$^{F/F}$;Akt-E17K* mice (n=4), we observed bioluminescence signals building up in half (2/4) of the injected mammary glands, due to activation of the oncogenic *Akt-E17K* allele (Supplementary Figure S5D). The luciferase-positive mammary glands showed tumors with typical ILC histology, expression of phospho-AKT^{Ser473} and CK8, and loss of E-cadherin, demonstrating that Cre expression from intraductally injected pSECC can give rise to ILC formation in predisposed mice (Figure 3B, Supplementary Figure S5E). We then sought to determine whether intraductal injection of pSECC-sg*Pten* into *Cdh1$^{F/F}$* mice (n=48) was sufficient to induce ILC. As a control, *Cdh1$^{F/F}$* mice were injected with pSECC-sgNT (n=27). Following sacrifice of the mice around 25 weeks post-injection, we observed tumors in 12 out of 48 *Cdh1$^{F/F}$* mammary glands injected with pSECC-sg*Pten* (Table 1). No lesions were observed in pSECC-sgNT injected *Cdh1$^{F/F}$* females. Notably, most tumors in pSECC-sg*Pten* injected *Cdh1$^{F/F}$* female mice were not classified as ILCs and were composed of both E-cadherin-negative and –positive cells, indicating incomplete Cre-mediated recombination of the *Cdh1^{F}* alleles (Figure 3C-D, Supplementary Figure S6A-B). The tumors were also strongly surrounded by infiltrating immune cells, which stained positive for CD4, CD8 and B220, indicating both T- and B-cell recruitment (Figure 3C). It was previously shown that somatic expression of Cas9 in adult mice may trigger Cas9-specific immune responses (Wang *et al.*, 2015). In an attempt to reduce immune recruitment, we tested whether transient immunosuppression by cyclosporin A administration (Howell *et al.*, 1998; Meuwissen *et al.*, 2001) would boost ILC development in pSECC-sg*Pten* injected *Cdh1$^{F/F}$* females, but this was not the case (*data not shown*). We obtained genomic DNA from tumor-bearing mammary glands

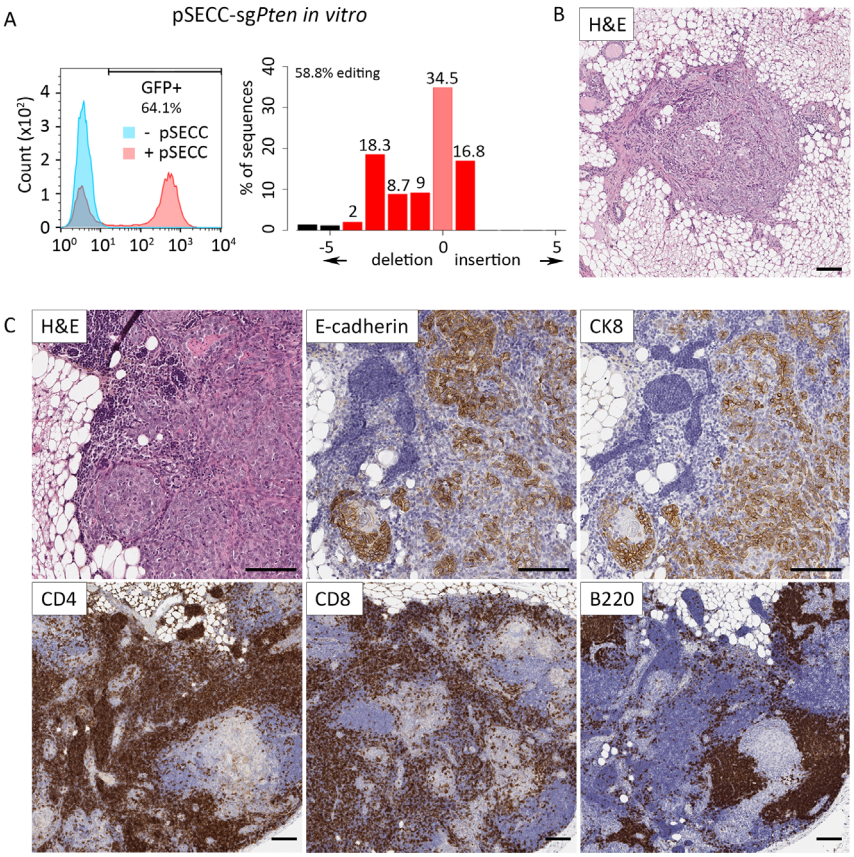

Figure 3 Intraductal injection of pSECC-sg*Pten* in *Cdh1*$^{F/F}$ mice results in non-ILC tumors with strong immune infiltrates. (A) Analysis of pSECC-sg*Pten*-transduced Cre-reporter cells 5 days after transduction. Percentage of GFP positive cells and the spectrum of insertions/deletions (indels) of the targeted *Pten* alleles are shown by FACS and TIDE analysis respectively. The fraction of unmodified alleles is depicted in pink, while red ($p<0.001$) and black ($p>0.001$) bars represent the fractions of modified alleles. (B) H&E staining of a representative tumor section from *Cdh1*$^{F/F}$*;Akt-E17K* mice injected with pSECC-sgNT (n=4). Tumors were analyzed 16 weeks after injection. Bar = 100 µm. (C) Immunohistochemical detection of E-cadherin, CK8, CD4, CD8 and B220 expressing cells in tumor sections from *Cdh1*$^{F/F}$ mice injected with pSECC-sg*Pten.* Tumor lesions were analyzed 25 weeks after injection. Bars = 100 µm. (D) Histological classification of tumors from *Cdh1*$^{F/F}$ mice injected with pSECC-sg*Pten* (n=48). ILC-like classification refers to lesions that are too small to display the typical ILC histological phenotype with the characteristic growth pattern. (E) TIDE analysis of the targeted *Pten* alleles in a representative tumor from pSECC-sg*Pten* injected *Cdh1*$^{F/F}$ mice.

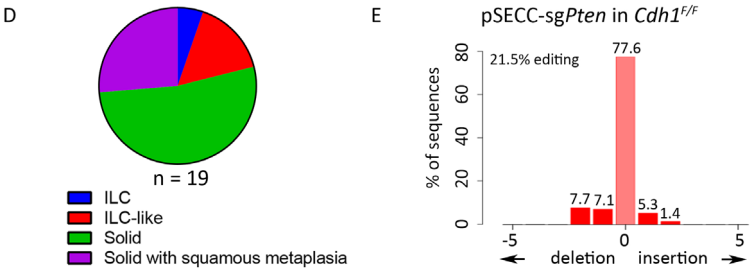

Figure 3 **Continued.** (D) Histological classification of tumors from *Cdh1*$^{F/F}$ mice injected with pSECC-sg*Pten* (n=48). ILC-like classification refers to lesions that are too small to display the typical ILC histological phenotype with the characteristic growth pattern. (E) TIDE analysis of the targeted *Pten* alleles in a representative tumor from pSECC-sg*Pten* injected *Cdh1*$^{F/F}$ mice.

Table 1 Overview of intraductal injections performed with pSECC and LentiGuide vectors, with affected mammary glands for each genotype.

Genotype	Vector	sgRNA	# injected mice	# injected glands	# affected glands	% affected glands
Cdh1$^{F/F}$	pSECC	sg*Pten*	26	48	12	25
Cdh1$^{F/F}$	pSECC	sgNT	14	27	0	0
WapCre;Cdh1$^{F/F}$*;Cas9*	LentiGuide	sg*Pten*	14	27	8	30
WapCre;Cdh1$^{F/F}$*;Cas9*	LentiGuide	sgNT	8	14	0	0
WapCre;Cdh1$^{F/F}$	LentiGuide	sg*Pten*	1	2	0	0
Cdh1$^{F/F}$*;Cas9*	LentiGuide	sg*Pten*	1	2	0	0

and confirmed target modification of *Pten* exon 1, resulting in frameshift mutations or larger deletions (Figure 3E, Supplementary Figure S6C). Indeed, immunofluorescence showed that tumors were PTEN negative, resulting in activation of PI3K/AKT signaling (Supplementary Figure S6A and S6D). Together, these data show that pSECC-mediated somatic Cre delivery and inactivation of *Pten* in mammary epithelial cells of *Cdh1*$^{F/F}$ mice induces tumors that do not resemble ILC and show a massive immune infiltrate. Importantly, Lenti-Cre mediated inactivation of *Pten* and E-cadherin in mammary glands of *Cdh1*$^{F/F}$*;Pten*$^{F/F}$ mice did not elicit a strong immune influx, suggesting that the immune infiltrate in tumors induced by pSECC is not due to somatic Cre expression (Supplementary Figure S4A).

Somatic gene editing and ILC formation in conditional Cas9 knock-in mice

Given that Cas9 was reported to be immunogenic (Wang *et al.*, 2015), we hypothesized that Cas9-specific immune responses might have limited the success of pSECC-sg*Pten* for ILC modeling in *Cdh1*$^{F/F}$ female mice. We therefore generated *Cdh1*$^{F/F}$;*Col1a1*$^{invCAG\text{-}Cas9\text{-}IRES\text{-}Luc/+}$ (*Cdh1*$^{F/F}$;*Cas9*) mice with a Cre-conditional *Cas9* allele in the *Col1a1* locus, as described above for the *Akt-E17K* mutant (Supplementary Figure S7A-B). Expression of Cre in mouse mammary epithelial cells (MMECs) derived from *Cdh1*$^{F/F}$;*Cas9* mice

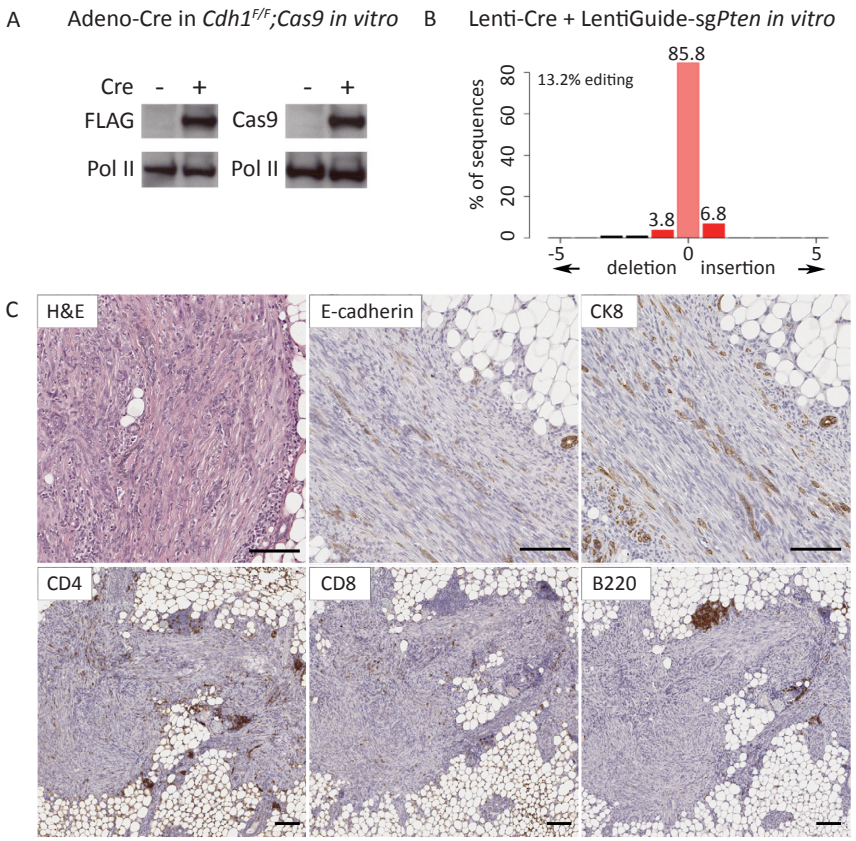

Figure 4 ILC formation in *WapCre;Cdh1*$^{F/F}$;*Cas9* mice injected with LentiGuide-sg*Pten*. (A) Expression of Cas9 from the Cre-conditional *Cas9* allele following *in vitro* transduction of *Cdh1*$^{F/F}$;*Cas9* MMECs with Adeno-Cre, as visualized by immunoblotting with anti-FLAG and anti-Cas9 antibodies. Pol II is shown as loading control. (B) TIDE analysis of the targeted *Pten* alleles in *Cdh1*$^{F/F}$;*Cas9* MMECs co-transduced with Lenti-Cre and LentiGuide-sg*Pten*. (C) Immunohistochemical detection of E-cadherin, CK8, CD4, CD8 and B220 expressing cells in tumor sections from *WapCre;Cdh1*$^{F/F}$;*Cas9* mice injected with LentiGuide-sg*Pten*. Tumor lesions were analyzed 25 weeks after injection. Bars = 100 μm.

induced the inversion of the CAG promoter and subsequent Cas9 protein expression (Figure 4A, Supplementary Figure S7C). To test the genomic editing capacity of the conditional *Cas9* knock-in allele, we made use of a lentiviral vector (LentiGuide) only encoding sg*Pten* or sgNT. Co-transduction of Lenti-Cre and LentiGuide-sg*Pten* vectors in MMECs derived from *Cdh1*$^{F/F}$*;Cas9* mice resulted in *Pten* gene editing in a fraction of cells (Figure 4B). No insertions/deletions (indels) at the targeted location were observed upon co-transduction of Lenti-Cre and LentiGuide-sgNT, or upon transduction with LentiGuide-sg*Pten* alone, thus validating the functionality of the conditional *Cas9* allele (Supplementary Figure S7D). To determine the utility of this approach for ILC modeling, we performed intraductal injections with LentiGuide-sg*Pten* (n=27) or LentiGuide-sgNT (n=14) in *WapCre;Cdh1*$^{F/F}$*;Cas9* female mice, which were analyzed for ILC development 25 weeks after injection. *Cdh1*$^{F/F}$*;Cas9* or *WapCre;Cdh1*$^{F/F}$ control mice injected with LentiGuide-sg*Pten*, or *WapCre;Cdh1*$^{F/F}$*;Cas9* mice injected with LentiGuide-sgNT did not display mammary tumor formation. In contrast, 8 out of 27 *WapCre;Cdh1*$^{F/F}$*;Cas9* mammary glands injected with LentiGuide-sg*Pten* developed one or more ILCs (Table 1, Supplementary Figure S8A-B). All tumors showed typical ILC histology, characterized by discohesive, CK8 positive and E-cadherin negative tumor

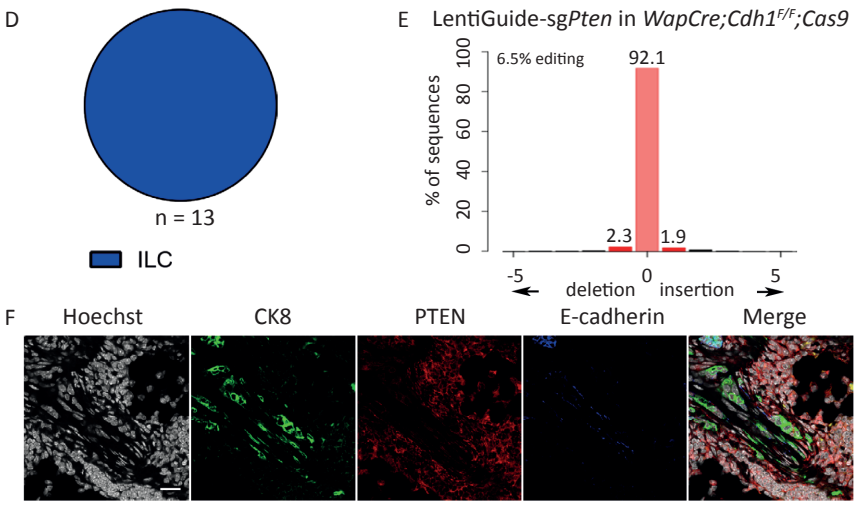

Figure 4 **Continued.** (D) Histological classification of tumors from *WapCre;Cdh1*$^{F/F}$*;Cas9* mice injected with LentiGuide-sg*Pten* (n=27). (E) TIDE analysis of the targeted *Pten* alleles in a representative tumor from LentiGuide-sg*Pten* injected *WapCre;Cdh1*$^{F/F}$*;Cas9*$^{F/F}$ mice. (F) Representative immunofluorescence imaging of tumor sections from LentiGuide-sg*Pten* injected *WapCre;Cdh1*$^{F/F}$*;Cas9* mice, stained with antibodies against CK8, PTEN and E-cadherin. Bar = 25 µm.

cells and an abundant presence of fibroblasts and collagen deposition (Figure 4C-D). Moreover, tumors showed an extent of immune infiltrate that was more limited than observed in the pSECC-sg*Pten* induced tumors and comparable to ILCs from Lenti-Cre injected *Cdh1*$^{F/F}$*;Pten*$^{F/F}$ mice (Figure 4C). These data suggest that *WapCre;Cdh1*$^{F/F}$*;Cas9* mice show immunological tolerance to *WapCre* driven Cas9 expression in mammary epithelium. This tolerance is likely caused by ectopic expression of Cas9 during early stages of postnatal development, induced by *WapCre* activity in brain (Supplementary Figure S9A-D; Wagner *et al.*, 1997). Target modification of *Pten* exon 1 was observed in genomic DNA from tumor-bearing mammary glands, and indels were exclusively frameshift mutations (Figure 4E, Supplementary Figure S8C). Consistent with this, tumors showed recombined *Cdh1*^{F} and *invCAG-Cas9-IRES-Luc* alleles, were positive for CK8 and negative for PTEN, E-cadherin and vimentin, and showed activation of PI3K/AKT signaling (Figure 4F, Supplementary Figure S8D-E). Collectively, these data show that intraductal delivery of sgRNA-*Pten* in *WapCre;Cdh1*$^{F/F}$*;Cas9* female mice induces ILCs that closely resemble tumors from *WapCre;Cdh1*$^{F/F}$*;Pten*$^{F/F}$ mice or Lenti-Cre injected *Cdh1*$^{F/F}$*;Pten*$^{F/F}$ mice. Moreover, preliminary data suggest that intraductal injection of *WapCre;Cdh1*$^{F/F}$*;Cas9* mice with a single lentiviral vector encoding two sgRNAs may allow for multiplex gene editing, which would enable *in vivo* validation of combinations of TSGs implicated in ILC (Supplementary Figure S10A-C).

Discussion

In this study we describe novel approaches for non-germline modeling of E-cadherin-deficient lobular breast carcinoma by the delivery of lentiviral vectors via intraductal injection in the nipples of adult female mice. By using high-titer lentiviral vector preparations, we achieved extensive transduction of the ductal system and *in vivo* Cre-mediated recombination when using Lenti-Cre preparations in *mT/mG* Cre-reporter mice. This recapitulates previous studies employing adenoviral vectors for somatic Cre delivery to murine mammary tissue (Tao *et al.*, 2014; Rutkowski *et al.*, 2014). We observed that the target cell population was composed of both CK8-positive luminal epithelial cells and CK14-positive basal cells. Intraductal administration of Lenti-Cre in the novel *Cdh1*$^{F/F}$*;Akt-E17K* and *Cdh1*$^{F/F}$*;Pten*$^{F/F}$ mouse models resulted in the transduction of ILC-initiating cells, as shown by the highly penetrant and rapid ILC development in these animals. Tumors developing in these mice were histologically indistinguishable from those arising in the *WapCre* based ILC models, suggesting that the cells targeted by intraductally injected lentiviruses are the same as the tumor-initiating cells in the spontaneous mouse models. Compared to the *WapCre*-driven model, Lenti-Cre injection simplifies breeding of experimental animals by eliminating the necessity of a Cre allele and allows a more sparse and stochastic targeting of ILC-initiating cells, better reflecting the sporadic nature of human cancer. Moreover, it allows spatiotemporal control of ILC initiation, and permits studying the initiating events of ILC in the adult mammary gland, whereas *WapCre* is already active during pre-puberal developmental stages. Furthermore, while transgenic animals often develop mammary tumors in multiple glands, tumor induction by intraductal injection can be restricted to a single gland, yielding *de novo* mammary tumor models suitable for studying development of metastatic disease following removal of the primary tumor and for evaluating efficacy of adjuvant systemic therapies.

A possible limitation of intraductal Cre delivery is the inherent lack of specificity of viral transduction, which might target also non-ILC-initiating cells in the mammary gland. Nonetheless, this promiscuity might be advantageous in case the cell-of-origin is unknown, and might enable modeling of other breast cancer subtypes by intraductal administration of Lenti-Cre to mice bearing different predisposing mutations, provided that the cells-of-origin for that tumor type can be transduced. Additionally, viral vectors in which Cre recombinase expression is driven by tissue-specific promoters might be used to target specific subtypes of mammary epithelial cells (Tao *et al.*, 2014).

Although intraductal injection of Lenti-Cre provides an effective approach to model breast cancer in mice, its applicability is dependent on the generation of effective conditional alleles for relevant oncogenes and tumor suppressors and their incorporation

in compound mice. An alternative approach that enables more rapid and methodic *in vivo* gene editing would be required to functionally validate the increasing numbers of candidate driver mutations that are being identified by genome-wide sequencing studies of human breast cancer (Cancer Genome Atlas Network, 2012; Stephens *et al.*, 2012; Ciriello *et al.*, 2015). The advent of CRISPR/Cas9-technologies allows for rapid somatic gene editing in nearly any cell type to study the effects of gene perturbation *in situ*. Several studies have already shown that tumor initiation and development in various tissues, including liver, lung, pancreas and brain, can be modeled *in vivo* by using CRISPR/Cas9-based somatic gene editing (Platt *et al.*, 2014; Sánchez-Rivera *et al.*, 2014; Xue *et al.*, 2014; Chiou *et al.*, 2015; Weber *et al.*, 2015; Zuckermann *et al.*, 2015). As a proof-of-concept, we performed intraductal injections with pSECC-sg*Pten* lentiviral vectors in *Cdh1*$^{F/F}$ female mice to simultaneously ablate E-cadherin expression and disrupt the TSG *Pten,* a negative regulator of PI3K/AKT signaling. While tumor lesions were observed in a limited number of animals, they did not resemble ILC and showed incomplete loss of E-cadherin, suggesting that tumorigenesis in *Cdh1*$^{F/F}$ mice injected with pSECC-sg*Pten* is driven by PTEN loss rather than by combined inactivation of both tumor suppressors. Moreover, all tumors in these mice showed a more profound immune infiltrate than the ILCs arising in Lenti-Cre injected *Cdh1*$^{F/F}$*;Pten*$^{F/F}$ animals, which might be due to humoral and cellular immunity against *S. pyogenes* Cas9 (Wang *et al.*, 2015), an aspect that thus far has been underappreciated in *in vivo* CRISPR/Cas9 studies. To avoid Cas9-directed immunity, we performed intraductal injections of LentiGuide-sg*Pten* in *WapCre;Cdh1*$^{F/F}$*;Cas9* female mice, which express the Cas9 endonuclease from a conditional knock-in allele in mammary epithelium. This resulted in E-cadherin negative tumor lesions resembling human ILC in 30% of the injected mammary glands upon a single administration of the lentiviral vector. Incomplete tumor penetrance could reflect reduced number of ILC-initiating cells in *WapCre;Cdh1*$^{F/F}$*;Cas9* female mice compared with wild-type mice, which might be due to the fact that E-cadherin loss in mammary epithelial cells induces apoptosis (Boussadia *et al.*, 2002). The lack of a massive immune infiltrate in these tumors indicates that conditional Cas9 expression in brain during early postnatal development leads to tolerance in *WapCre;Cdh1*$^{F/F}$*;Cas9* mice, resulting in efficient ILC development following CRISPR/Cas9-mediated disruption of the *Pten* alleles. Indeed, TIDE (tracking of indels by decomposition) analyses of tumor-bearing mammary glands exclusively showed frame-shifting genetic alterations in *Pten* and concomitant activation of phospho-AKT^{Ser473}, indicating positive selection for cells with disrupted PTEN in E-cadherin-deficient cells and providing functional support for the notion that activating mutations in the PI3K/AKT signaling pathway and inactivating mutations in *CDH1* effectively collaborate in human ILC development.

Taken together, we have shown for the first time that CRISPR/Cas9-mediated somatic gene editing of mammary epithelial cells can be used to target and genetically modify

ILC-initiating cells by intraductal injection of sgRNA-encoding lentiviral vectors in *WapCre;Cdh1$^{F/F}$;Cas9* female mice. This approach allows rapid *in vivo* testing of putative co-occurring mutations with E-cadherin loss to initiate invasive lobular breast carcinoma and could in principle be extended to other breast cancer subtypes. Our preliminary data with single lentiviral vectors encoding multiple sgRNAs suggest that *WapCre;Cdh1$^{F/F}$;Cas9* mice may be used for multiplex gene editing of the mammary gland, in order to test combinations of TSGs implicated in ILC. It will be interesting to determine whether *WapCre;Cdh1$^{F/F}$;Cas9* mice may also be used for *in vivo* forward genetic screens with focused CRISPR libraries to identify novel TSGs critical for ILC development. To test candidate drivers that are overexpressed or amplified in ILC, it may be relevant to develop *WapCre;Cdh1$^{F/F}$;dCas9-p300core* mice with conditional expression of nuclease-deficient Cas9 fused to the catalytic core of the human acetyltransferase p300 (Hilton *et al.*, 2015).

Acknowledgements

We are grateful to Marco Barazas, Chiara Brambillasca, Bastiaan Evers, Francisco J. Sánchez-Rivera, Tyler Jacks, Lorenzo Bombardelli, Ingrid van der Heijden, Ellen Wientjens, Renske de Korte-Grimmerink and Natalie Proost for providing valuable reagents, technical suggestions and/or help with the experiments, and to Jelle Wesseling for critical reading of the manuscript. We thank the NKI animal facility, animal pathology facility, Core Facility Molecular Pathology & Biobanking (CFMPB), flow cytometry facility and genomics core facility for their expert technical support. Financial support was provided by the Netherlands Organization for Scientific Research (NWO: Cancer Genomics Netherlands (CGCNL), Cancer Systems Biology Center (CSBC), VENI 016156012 to MN, NGI Zenith 93512009 and VICI 91814643 to JJ), Worldwide Cancer Research (grant 14-0288 to JJ and MHvM), the EU Seventh Framework Program (EurocanPlatform project 260791 and Infrafrontier-I3 project 312325), the European Research Council (ERC Synergy project CombatCancer), and a National Roadmap grant for Large-Scale Research Facilities from the NWO.

References

Boelens MC, Nethe M, Klarenbeek S, Bonzanni N, Zeeman A, Wientjens E, Schut E, Drenth A, van der Burg E, Boon U, et al. 2016. PTEN loss rescues apoptosis in E-cadherin deficient mammary epithelial cells, resulting in development of classical invasive lobular carcinoma in mice. Cell reports 16: 2087-101.

Borst MJ, Ingold JA. 1993. Metastatic patterns of invasive lobular versus invasive ductal carcinoma of the breast. Surgery 114: 637–641.

Boussadia O, Kutsch S, Hierholzer A, Delmas V, Kemler R. 2002. E-cadherin is a survival factor for the lactating mouse mammary gland. Mech Dev 115: 53–62.

Brinkman EK, Chen T, Amendola M, van Steensel B. 2014. Easy quantitative assessment of genome editing by sequence trace decomposition. Nucleic Acids Res 42: 168.

Cancer Genome Atlas Network. 2012. Comprehensive molecular portraits of human breast tumours. Nature 490: 61–70.

Cardiff RD, Anver MR, Gusterson BA, Hennighausen L, Jensen RA, Merino MJ, Rehm S, Russo J, Tavassoli FA, Wakefield LM, et al. 2000. The mammary pathology of genetically engineered mice: the consensus report and recommendations from the Annapolis meeting. Oncogene 19: 968–988.

Chiou S-H, Winters IP, Wang J, Naranjo S, Dudgeon C, Tamburini FB, Brady JJ, Yang D, Grüner BM, Chuang C-H, et al. 2015. Pancreatic cancer modeling using retrograde viral vector delivery and in vivo CRISPR/Cas9-mediated somatic genome editing. Genes Dev 29: 1576–1585.

Ciriello G, Gatza ML, Beck AH, Wilkerson MD, Rhie SK, Pastore A, Zhang H, McLellan M, Yau C, Kandoth C, et al. 2015. Comprehensive Molecular Portraits of Invasive Lobular Breast Cancer. Cell 163: 506–519.

Derksen PWB, Braumuller TM, van der Burg E, Hornsveld M, Mesman E, Wesseling J, Krimpenfort P, Jonkers J. 2011. Mammary-specific inactivation of E-cadherin and p53 impairs functional gland development and leads to pleomorphic invasive lobular carcinoma in mice. Dis Model Mech 4: 347–358.

Derksen PWB, Liu X, Saridin F, van der Gulden H, Zevenhoven J, Evers B, van Beijnum JR, Griffioen AW, Vink J, Krimpenfort P, et al. 2006. Somatic inactivation of E-cadherin and p53 in mice leads to metastatic lobular mammary carcinoma through induction of anoikis resistance and angiogenesis. Cancer Cell 10: 437–449.

Doornebal CW, Klarenbeek S, Braumuller TM, Klijn CN, Ciampricotti M, Hau C-S, Hollmann MW, Jonkers J, de Visser KE. 2013. A preclinical mouse model of invasive lobular breast cancer metastasis. Cancer Res 73: 353–363.

Droufakou S, Deshmane V, Roylance R, Hanby A, Tomlinson I, Hart IR. 2001. Multiple ways of silencing E-cadherin gene expression in lobular carcinoma of the breast. Int J Cancer 92: 404–408.

Ewald AJ, Brenot A, Duong M, Chan BS, Werb Z. 2008. Collective epithelial migration and cell rearrangements drive mammary branching morphogenesis. Dev Cell 14: 570–581.

Follenzi A, Ailles LE, Bakovic S, Geuna M, Naldini L. 2000. Gene transfer by lentiviral vectors is limited by nuclear translocation and rescued by HIV-1 pol sequences. Nat Genet 25: 217–222.

Harada N, Oshima H, Katoh M, Tamai Y, Oshima M, Taketo MM. 2004. Hepatocarcinogenesis in mice with beta-catenin and Ha-ras gene mutations. Cancer Res 64: 48–54.

Henneman L, van Miltenburg MH, Michalak EM, Braumuller TM, Jaspers JE, Drenth AP, de Korte-Grimmerink R, Gogola E, Szuhai K, Schlicker A, et al. 2015. Selective resistance to the PARP inhibitor olaparib in a mouse model for BRCA1-deficient metaplastic breast cancer. Proc Natl Acad Sci USA 112: 8409–8414.

Hilton IB, D'Ippolito AM, Vockley CM, Thakore PI, Crawford GE, Reddy TE, Gersbach CA. 2015. Epigenome editing by a CRISPR-Cas9-based acetyltransferase activates genes from promoters and enhancers. Nat Biotechnol 33: 510–517.

Howell JM, Lochmüller H, O'Hara A, Fletcher S, Kakulas BA, Massie B, Nalbantoglu J, Karpati G. 1998. High-level dystrophin expression after adenovirus-mediated dystrophin minigene transfer to skeletal muscle of dystrophic dogs: prolongation of expression with immunosuppression. Hum Gene Ther 9: 629–634.

Huijbers IJ, Bin Ali R, Pritchard C, Cozijnsen M, Kwon M-C, Proost N, Song J-Y, de Vries H, Badhai J, Sutherland K, et al. 2014. Rapid target gene validation in complex cancer mouse models using re-derived embryonic stem cells. EMBO Molecular Medicine 6: 212-225.

Huijbers IJ, Del Bravo J, Bin Ali R, Pritchard C, Braumuller TM, van Miltenburg MH, Henneman L, Michalak EM, Berns A, Jonkers J. 2015. Using the GEMM-ESC strategy to study gene function in mouse models. Nature Protocols 10: 1755–1785.

Kirsch DG, Dinulescu DM, Miller JB, Grimm J, Santiago PM, Young NP, Nielsen GP, Quade BJ, Chaber CJ, Schultz CP, et al. 2007. A spatially and temporally restricted mouse model of soft tissue sarcoma. Nat Med 13: 992–997.

Krause S, Brock A, Ingber DE. 2013. Intraductal injection for localized drug delivery to the mouse mammary gland. J Vis Exp. 80: 50692.

Marino S, Krimpenfort P, Leung C, van der Korput HAGM, Trapman J, Camenisch I, Berns A, Brandner S. 2002. PTEN is essential for cell migration but not for fate determination and tumourigenesis in the cerebellum. Development 129: 3513–3522.

Martinez V, Azzopardi JG. 1979. Invasive lobular carcinoma of the breast: incidence and variants. Histopathology 3: 467–488.

Meuwissen R, Linn SC, van der Valk M, Mooi WJ, Berns A. 2001. Mouse model for lung tumorigenesis through Cre/lox controlled sporadic activation of the K-Ras oncogene. Oncogene 20: 6551–6558.

Moll R, Mitze M, Frixen UH, Birchmeier W. 1993. Differential loss of E-cadherin expression in infiltrating ductal and lobular breast carcinomas. Am J Pathol 143: 1731–1742.

Muzumdar MD, Tasic B, Miyamichi K, Li L, Luo L. 2007. A global double-fluorescent Cre reporter mouse. Genesis 45: 593–605.

Pasic L, Eisinger-Mathason TSK, Velayudhan BT, Moskaluk CA, Brenin DR, Macara IG, Lannigan DA. 2011. Sustained activation of the HER1-ERK1/2-RSK signaling pathway controls myoepithelial cell fate in human mammary tissue. Genes Dev 25: 1641–1653.

Platt RJ, Chen S, Zhou Y, Yim MJ, Swiech L, Kempton HR, Dahlman JE, Parnas O, Eisenhaure TM, Jovanovic M, et al. 2014. CRISPR-Cas9 knockin mice for genome editing and cancer modeling. Cell 159: 440–455.

Rakha EA, Patel A, Powe DG, Benhasouna A, Green AR, Lambros MB, Reis-Filho JS, Ellis IO. 2010. Clinical and biological significance of E-cadherin protein expression in invasive lobular carcinoma of the breast. Am J Surg Pathol 34: 1472–1479.

Russell TD, Fischer A, Beeman NE, Freed EF, Neville MC, Schaack J. 2003. Transduction of the mammary epithelium with adenovirus vectors in vivo. J Virol 77: 5801–5809.

Rutkowski MR, Allegrezza MJ, Svoronos N, Tesone AJ, Stephen TL, Perales-Puchalt A, Nguyen J, Zhang PJ, Fiering SN, Tchou J, et al. 2014. Initiation of metastatic breast carcinoma by targeting of the ductal epithelium with adenovirus-cre: a novel transgenic mouse model of breast cancer. J Vis Exp. 85: 51171.

Sánchez-Rivera FJ, Papagiannakopoulos T, Romero R, Tammela T, Bauer MR, Bhutkar A, Joshi NS, Subbaraj L, Bronson RT, Xue W, et al. 2014. Rapid modelling of cooperating genetic events in cancer through somatic genome editing. Nature 516: 428–431.

Sanjana NE, Shalem O, Zhang F. 2014. Improved vectors and genome-wide libraries for CRISPR screening. Nat Methods 11: 783–784.

Tao L, van Bragt MPA, Laudadio E, Li Z. 2014. Lineage tracing of mammary epithelial cells using cell-type-specific cre-expressing adenoviruses. Stem Cell Reports 2: 770–779.

Vos CB, Cleton-Jansen AM, Berx G, de Leeuw WJ, ter Haar NT, van Roy F, Cornelisse CJ, Peterse JL, van de Vijver MJ. 1997. E-cadherin inactivation in lobular carcinoma in situ of the breast: an early event in tumorigenesis. Br J Cancer 76: 1131–1133.

Wagner KU, Wall RJ, St-Onge L, Gruss P, Wynshaw-Boris A, Garrett L, Li M, Furth PA, Hennighausen L. 1997. Cre-mediated gene deletion in the mammary gland. Nucleic Acids Res 25: 4323–4330.

Wang D, Mou H, Li S, Li Y, Hough S, Tran K, Li J, Yin H, Anderson DG, Sontheimer EJ, et al. 2015. Adenovirus-Mediated Somatic Genome Editing of Pten by CRISPR/Cas9 in Mouse Liver in Spite of Cas9-Specific Immune Responses. Hum Gene Ther 26: 432–442.

Weber J, Öllinger R, Friedrich M, Ehmer U, Barenboim M, Steiger K, Heid I, Mueller S, Maresch R, Engleitner T, et al. 2015. CRISPR/Cas9 somatic multiplex-mutagenesis for high-throughput functional cancer genomics in mice. Proc Natl Acad Sci USA 112: 13982–13987.

Wong H, Lau S, Cheung P, Wong TT, Parker A, Yau T, Epstein RJ. 2014. Lobular breast cancers lack the inverse relationship between ER/PR status and cell growth rate characteristic of ductal cancers in two independent patient cohorts: implications for tumor biology and adjuvant therapy. BMC Cancer 14: 826.

Xue W, Chen S, Yin H, Tammela T, Papagiannakopoulos T, Joshi NS, Cai W, Yang G, Bronson R, Crowley DG, et al. 2014. CRISPR-mediated direct mutation of cancer genes in the mouse liver. Nature 514: 380–384.

Zuckermann M, Hovestadt V, Knobbe-Thomsen CB, Zapatka M, Northcott PA, Schramm K, Belic J, Jones DTW, Tschida B, Moriarity B, et al. 2015. Somatic CRISPR/Cas9-mediated tumour suppressor disruption enables versatile brain tumour modelling. Nat Commun 6: 7391.

Materials and Methods

Lentiviral vectors

The LentiGuide vector was a kind gift from Feng Zhang (Addgene plasmid #52963). The pSECC vector was a kind gift from Tyler Jacks (Addgene plasmid #60820). The sgRNA targeting *Pten* exon 1 (GCTAACGATCTCTTTGATGA) is the validated gRNA used in (Sánchez-Rivera *et al.*, 2014), while the non-targeting gRNA (TGATTGGGGGTCGTTCGCCA) was selected from the list of non-targeting gRNAs of the GeCKO v2 mouse gRNA library (Sanjana *et al.*, 2014). Cloning of gRNAs in LentiGuide and pSECC was performed as described (Sanjana *et al.*, 2014). Tandem sgRNA vectors were made by cloning in tandem either two non-targeting sgRNA expression cassettes or the *Pten* gRNA expression cassette followed by a gRNA expression cassette targeting *Trp53* exon 5 (GAAGTCACAGCACATGACGG) (Evers *et al.*, *in preparation*). All vectors were validated by Sanger sequencing. Lenti-Cre (pBOB-CAG-iCRE-SD, Addgene plasmid #12336) was a kind gift of Lorenzo Bombardelli. We produced concentrated lentiviral stocks, pseudotyped with the VSV-G envelope, by transient co-transfection of four plasmids in 293T cells as previously described (Follenzi *et al.*, 2000). Viral titers were determined using the qPCR lentivirus titration kit from Abm (LV900).

Cell culture

Mouse mammary epithelial cells (MMECs) were isolated from 12 weeks old females as previously described (Ewald *et al.*, 2008) and cultured in DMEM-F12 medium containing 10% fetal bovine serum (FBS), 100 IU/ml penicillin, 100 µg/ml streptomycin, 5 ng/ml insulin, 5 ng/ml epidermal growth factor (EGF) (all Life Technologies), and 5 ng/ml cholera toxin (Sigma). 293T cells for lentiviral production and the Cre-reporter 293T cell line (containing a lox-stop-lox-GFP cassette) were cultured in Iscove's medium (Life Technologies) containing 10% FBS, 100 IU/ml penicillin, and 100 µg/ml streptomycin. Transductions were performed by adding diluted viral supernatant to the cells in the presence of 8 µg/mL polybrene (Sigma). Cells were transduced at multiplicity of infection (MOI) 10 for 24 hours, after which medium was refreshed. Harvesting of cells for flow cytometry and/or genomic DNA isolation was performed 5 days after transduction.

Flow cytometry

Cells were collected 5 days after transduction and directly analyzed for GFP fluorescence using a Becton Dickinson FACSCalibur. Viable cells were gated on size and shape using forward and side scatter. GFP expression was measured using a 488 nm excitation laser. Data analysis was performed using FlowJo software version 7.6.5.

Genomic DNA isolation, PCR amplification and TIDE analysis

Genomic DNA from frozen cell pellets and mammary gland frozen pieces was isolated using the Gentra Puregene genomic DNA isolation kit from Qiagen. PCR amplification of *Pten* exon 1 or *Trp53* exon 5 was performed with specific primers spanning the target site (FW_*Pten*: GCCCAGTCTCTGCAACCATC; RV_*Pten*: CACGATCTAGAAATGCGCCC; FW_*Trp53:* CCCACCTTGACACCTGATCG; RV_*Trp53:* CCACCCGGATAAGATGCTGG) and 1 µg DNA template, using the Q5 high-fidelity PCR kit from NEB. Amplicons were run on 1% agarose gel and gel purification was performed using the Isolate II PCR and Gel kit from Bioline. PCR products were Sanger sequenced using the FW primer and CRISPR/Cas9-induced editing efficacy was quantified with the TIDE algorithm as described (Brinkman *et al.*, 2014; http://tide.nki.nl). Non-transduced cells were used as a negative control in all genomic DNA amplifications, and only TIDE outputs with R^2>0.9 were considered. Inversion of the CAG promoter (Huijbers *et al.*, 2015) of the *Akt-E17K*-conditional allele was detected as described (Huijbers *et al.*, 2014) with a shared FW primer located on Lox66 (primer 1: GGCCGGCCATAACTTCGTATAATG) and two RV primers, one located in the vector backbone (primer 2: CTGCGTTATCCCCTGATTCTGTGG) to detect the non-recombined allele (product size: 897 bp) and one in the Hygromycin-B resistance gene (primer 3: CCTACATCGAAGCTGAAAGCACGAG) to identify the recombined allele (product size: 1054 bp). Inversion of the CAG promoter of the *Cas9*-conditional allele was detected using the Q5 kit to amplify the *Col1a1* locus with a shared FW primer located on the CAG promoter itself (primer 1: CTTCTCCCTCTCCAGCCTCGGG) and two RV primers, one located on the Hygromycin-B resistance gene (primer 2: CATCAGGTCGGAGACGCTGTCG) and one on the Cas9 shuttle (primer 3: TCGACGGATCTTGGGAGGCCTA). PCR amplification with primers 1 and 2 identifies a band of 386 bp, the non-recombined shuttle construct. PCR amplification with primers 1 and 3 identifies a band of 264 bp, when Cre-mediated recombination of the shuttle construct has occurred. $Cdh1^{F}$ and $Cdh1^{\Delta}$, alleles were identified by PCR as described (Derksen *et al.*, 2006). $Pten^{F}$ alleles were detected by PCR using primers located in intron 5 (FW: TGGGGGTATTCACTAGTATAG and RV: GAGTCCTCT-GAAAAAGCAGTC; product size: 200 bp). $Pten^{\Delta}$ alleles were detected using a FW primer in intron 4 (CCTAGGCTACTGCTCATT) and the RV primer located in intron 5 (product size: 350 bp). The tandem vector was detected using the Q5 high-fidelity PCR kit from NEB. FW primer is located at the human U6 promoter (primer 1: CAAAGATATTAGTACAAAATA-CGT) and RV primer at the SFFV promoter (primer 2: TGAACTTCTCTATTCTTGGTTTGGT; product size: 831 bp).

Adeno-Cre transduction in vitro

MMECs were seeded in six-well plates and confluent wells were transduced with viral Ad5-CMV-Cre particles (1×10^8 Transducing Units (TU); Gene Transfer Vector Core,

University of Iowa) in the presence of 8 µg/ml polybrene (Sigma). Five days after transduction DNA and proteins were isolated.

Immunoblotting

Protein lysates were made using lysis buffer (20 mM Tris pH 8.0, 300 mM NaCl, 2% NP40, 20% glycerol, 10 mM EDTA) complemented with protease inhibitors (Roche) and quantified using the BCA Protein Assay Kit (Pierce). Protein lysate was loaded onto a 3%–8% Tris-acetate gradient gel (Invitrogen) and transferred overnight onto PVDF membrane (Millipore) in transfer buffer (238 mM glycine, 80 mM TRIS and 0.01% SDS in water). Membranes were blocked in 5% ELK in PBS-T (0.05% Tween-20) after which they were stained for four hours at room temperature using the primary antibodies anti-FLAG (1:1000, Sigma Aldrich F1804) and anti-Cas9 (1:1000, Cell Signaling #14697) in 1% ELK in PBS-T. Pol II (1:400, Santa Cruz sc-5943) was incubated for 1 hr at room temperature in 1% ELK in PBS-T. Membranes were washed three times with 1% ELK in PBS-T and incubated for 1 hr with an HRP-conjugated secondary antibody (1:2000, DAKO). Stained membranes were washed three times in 1% ELK in PBS-T and then developed using SuperSignal ECL (Pierce).

Mice

Akt1 cDNA (Open Biosystems; #100067520) was modified using site-directed mutagenesis (Agilent QuikChange Lightning Multi Kit; FW: GCTGCAC AAACGAGGGAAGTACATCAAGACCTG, RV: CAGGTCTTGATGTACTTCCCTCGTTTGTGCAGC) resulting in mutant *Akt-E17K*. *Akt-E17K* and *Cas9* (Addgene plasmid #42229) cDNAs were sequence verified and inserted as respectively FseI-PmeI and BamHI fragments into the *Frt-invCag-IRES-Luc* vector, resulting in *Frt-invCag-AktE17K-IRES-Luc* and *Frt-invCag-Cas9-IRES-Luc*. Flp-mediated integration of the shuttle vectors in *WapCre;Cdh1$^{F/F}$;Col1a1$^{frt/+}$* GEMM-ESC clones was performed as described (Huijbers *et al.*, 2015). Chimeric animals were crossed with *WapCre;Cdh1$^{F/F}$* and *Cdh1$^{F/F}$* animals to generate the cohorts. *WapCre, Cdh1^{F}*, *mT/mG*, *Col1a1$^{invCAG\text{-}AktE17K\text{-}IRES\text{-}Luc}$* and *Col1a1$^{invCAG\text{-}Cas9\text{-}IRES\text{-}Luc}$* alleles were detected using PCR as described (Derksen *et al.*, 2006; Derksen *et al.*, 2011; Muzumdar *et al.*, 2007; Huijbers *et al.*, 2014). *Pten^{F}* alleles were detected by standard PCR at annealing temperature of 58°C using primers located in intron 5 (FW: TGGGGGTATTCACTAGTATAG and RV: GAGTCCTCTGAAAAAGCAGTC; product size: 200 bp) (Marino *et al.*, 2002).

In vivo bioluminescence imaging

In vivo bioluminescence imaging was performed as described (Henneman *et al.*, 2015) by using a cooled CCD system (Xenogen Corp., CA, USA) coupled to Living Image acquisition and analysis software (Xenogen). Signal intensity was measured over the region of interest and quantified as Flux (photons/sec/cm^2/sr).

Intraductal injections

Intraductal injections were performed as described (Krause *et al.*, 2013). Briefly, the mice were anesthetized using ketamine/sedazine (100 and 10 mg/kg respectively) and hair was removed in the nipple area with a commercial hair removal cream. 18 µl of high-titer lentivirus (or adenovirus) mixed with 2 µl 0.2% Evans blue dye in PBS was injected in the fourth mammary glands by using a 34-gauge needle. Mice were handled in a biological safety cabinet under a stereoscope. Lentiviral titers ranging from $2x10^8$ TU/mL to $2x10^9$ TU/mL were used. Animal experiments were approved by the Animal Ethics Committee of the Netherlands Cancer Institute and performed in accordance with institutional, national and European guidelines for Animal Care and Use.

Fluorescence imaging of freshly isolated tissue

FVB mice injected with Lenti-GFP, *mT/mG* animals injected with Lenti-Cre, and *mT/mG* mice injected with Adeno-Cre, were sacrificed 3 days or 2 weeks post-injection. Mammary glands were isolated and kept in PBS on ice prior to imaging. The brains and the mammary glands of the *WapCre;mT/mG* pups were isolated at the indicated time points. Images were acquired by using the Zeiss AxioZoom.V16 Stereo Microscope and were analyzed by the ZEN lite 2012 (Blue edition) software.

Histology and immunohistochemistry

Tissues were formalin-fixed and paraffin-embedded by routine procedures. H&E staining was performed as described (Doornebal *et al.*, 2013). Five semi-serial slides per injected mammary gland were stained with H&E, and reviewed by a blinded and dedicated pathologist (S. Klarenbeek) according to international consensus of mammary pathology (Cardiff *et al.*, 2000). Quantitation of the number of tumors per gland was performed using a single H&E stained slide per mammary gland. Tumor burden was calculated as the ratio between the total tumor area and the area of the whole mammary gland using ImageJ software version 1.4.3.67. Immunohistochemical stainings were processed as described (Doornebal *et al.*, 2013; Henneman *et al.*, 2015). All slides were digitally processed using the Aperio ScanScope (Aperio, Vista, CA, USA) and captured using ImageScope software version 12.0.0 (Aperio).

Immunofluorescence

Formalin-fixed and paraffin-embedded sections were processed as described (Pasic et al., 2011). Sections were incubated overnight at 4°C with primary antibodies anti-cytokeratin 8 (1:100, University of Iowa TROMA-1), anti-cytokeratin 14 (1:200, Covance #PRB-155P), anti-PTEN (1:100, Cell Signaling #9188) and anti-E-cadherin (1:100, BD Biosciences #610181). Secondary antibodies anti-Rat-AlexaFluor 647 (1:1000, Invitrogen #A21247), anti-Rabbit-AlexaFluor 568 (1:1000, Invitrogen #A11011) and anti-Mouse-AlexaFluor 488 (1:1000, Molecular Probes #A21141) were incubated overnight at 4°C. Sections were subsequently stained with Hoechst (1:1000, Thermo Scientific #62249) for 5 min and mounted using Vectashield (Vector Laboratories H-1000). Images were acquired using a Leica TCS SP5 Confocal and were analyzed using LAS AF Version 2.6.3 software.

Supplementary Figure legends

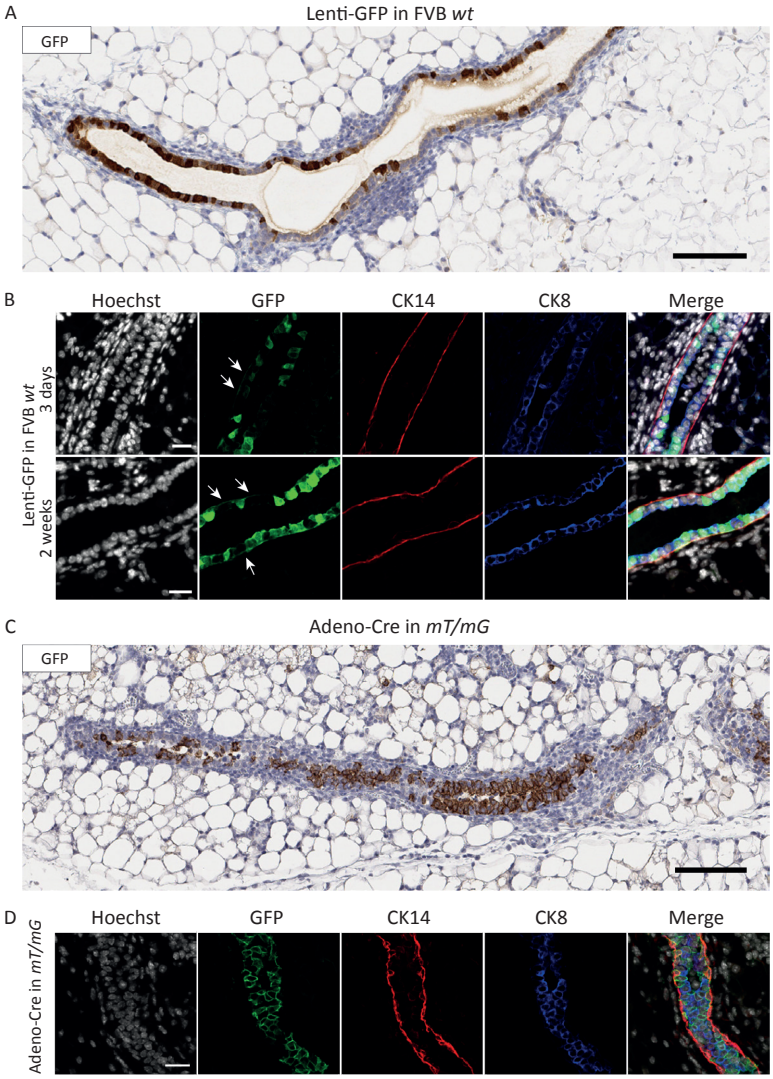

Supplementary Figure S1
Intraductal injections of Lenti-GFP in FVB wild-type animals and Adeno-Cre in double-fluorescent *mT/mG* Cre-reporter mice. (A) Immunohistochemistry of GFP expression in a representative mammary gland section of FVB wild-type mice after intraductal injection of Lenti-GFP (n=8). Mice were analyzed 14 days after injection. Bar = 100 µm. (B) Immunofluorescence analysis of GFP, CK8 and CK14 in mammary gland sections from Lenti-GFP injected FVB mice, showing GFP expression in CK8 positive luminal epithelial cells and CK14 positive basal cells (with arrowheads). Bars = 25 µm. Mice were analyzed at the indicated time points after injection. (C) Immunohistochemistry of GFP expression in a representative mammary gland section of *mT/mG* Cre-reporter mice intraductally injected with Adeno-Cre (n=8). Mice were analyzed 14 days after injection. Bar = 100 µm. (D) Immunofluorescence analysis of GFP, CK8 and CK14 in mammary gland sections from Adeno-Cre injected *mT/mG* Cre-reporter mice, showing GFP expression upon Cre-recombination. Bar = 25 µm.

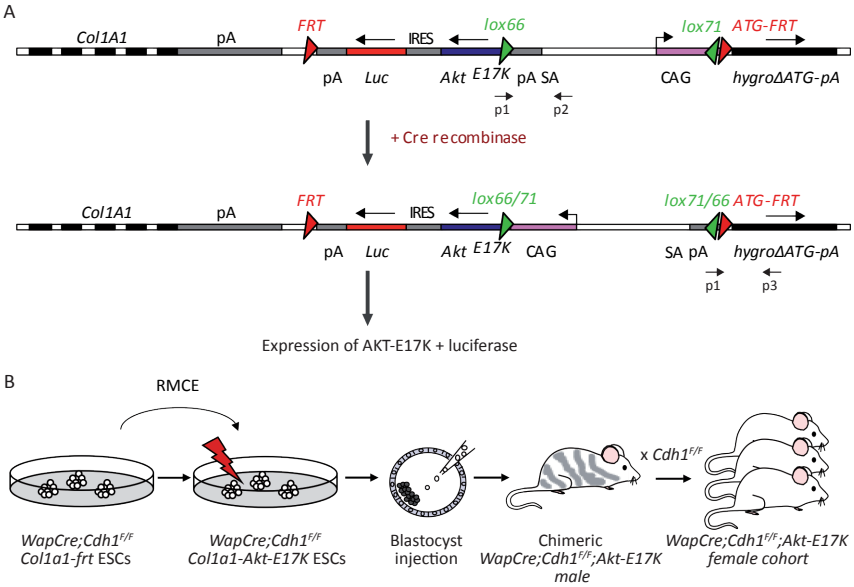

Supplementary Figure S2

Schematic overview of the GEMM-ESC strategy. (A) Depiction of the Cre-conditional *invCAG-AktE17K-IRES-Luc* allele integrated into the *Col1a1* locus of embryonic stem cells (ESCs) derived from *WapCre;Cdh1$^{F/F}$* mice. WapCre-mediated recombination allows mammary-specific inversion of the CAG promoter, resulting in expression of the oncogenic AKT-E17K variant accompanied by luciferase expression. (B) Chimeric mice were generated upon blastocyst injection of the modified ESCs. High-quality male chimeras were mated with *Cdh1$^{F/F}$* females to generate a cohort of *WapCre;Cdh1$^{F/F}$;Col1a1$^{invCAG\text{-}AktE17K\text{-}IRES\text{-}Luc/+}$* (*WapCre;Cdh1$^{F/F}$;Akt-E17K*) female mice.

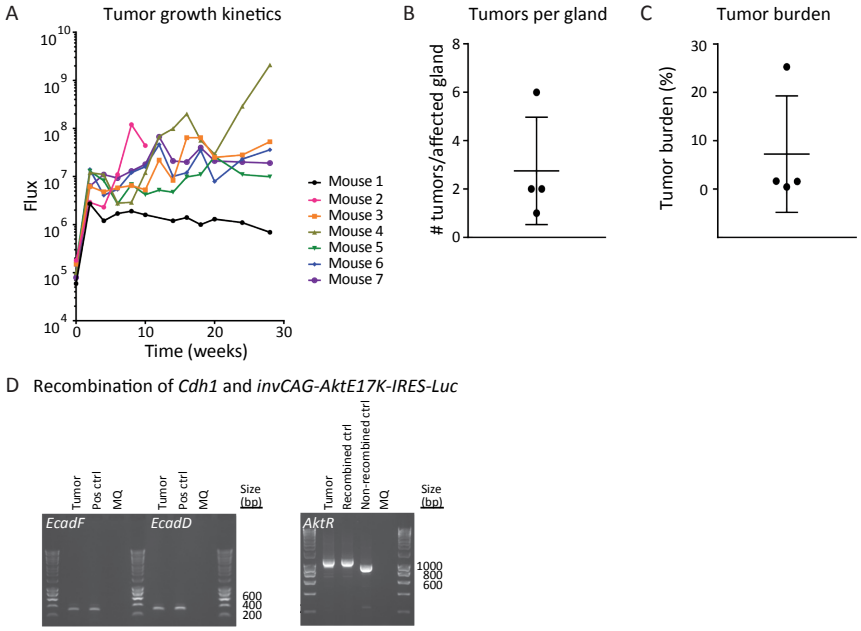

Supplementary Figure S3

Analysis of mammary tumors in *Cdh1*$^{F/F}$*;Akt-E17K* mice injected with Lenti-Cre. (A) Longitudinal *in vivo* bioluminescence imaging of luciferase expression in *Cdh1*$^{F/F}$*;Akt-E17K* animals injected with Lenti-Cre (n=7), showing signal build-up over time except for mouse 1, which did not develop a mammary tumor. (B) Box plot showing numbers of tumors detected in each affected mammary gland of *Cdh1*$^{F/F}$*;Akt-E17K* mice injected with Lenti-Cre. Mammary glands were harvested and analyzed 30 weeks after injection. (C) Box plot showing tumor burden in each affected mammary gland of *Cdh1*$^{F/F}$*;Akt-E17K* mice injected with Lenti-Cre. (D) Recombination status of the Cre-conditional *Akt-E17K* allele and *Cdh1* alleles in a Lenti-Cre induced *Cdh1*$^{F/F}$*;Akt-E17K* tumor, as visualized by PCR. EcadF and EcadD are PCRs to detect the *Cdh1*^{F} or *Cdh1*$^{\Delta}$ alleles, respectively. AktR detects the recombined (1054 bp) and non-recombined (897 bp) Cre-conditional *Akt-E17K* allele (primer positions are shown in Supplementary Figure S2A).

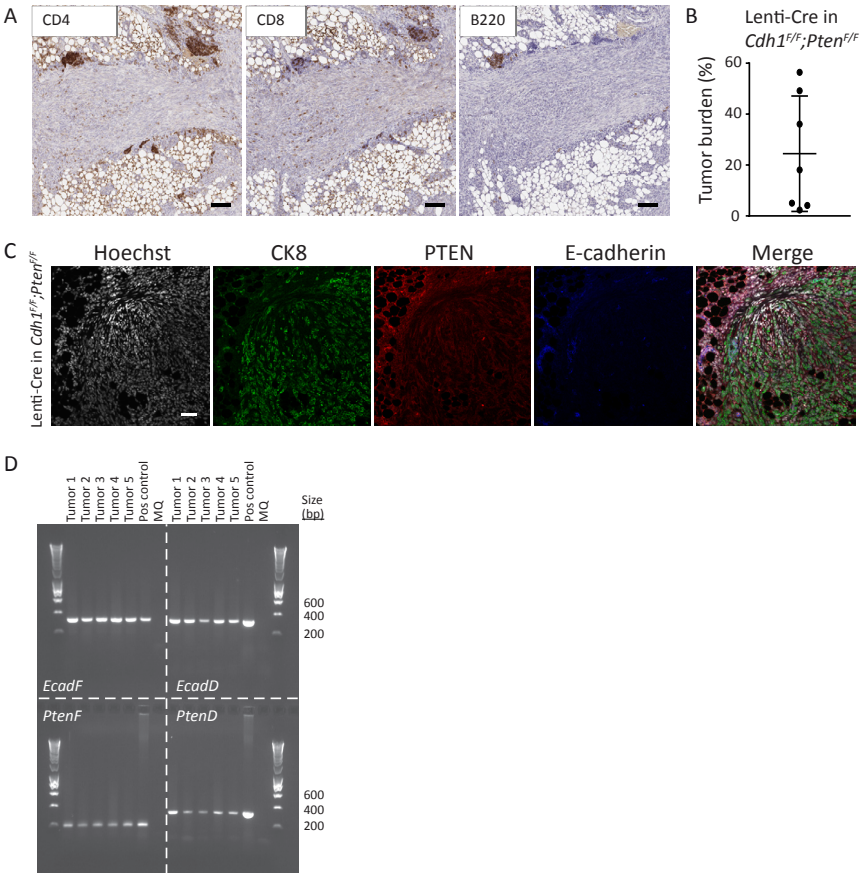

Supplementary Figure S4

Analysis of mammary gland tumors in *Cdh1*$^{F/F}$;*Pten*$^{F/F}$ mice injected with Lenti-Cre. (A) Immunohistochemical detection of CD4, CD8 and B220 expressing cells in tumor sections from *Cdh1*$^{F/F}$;*Pten*$^{F/F}$ mice injected with Lenti-Cre (n=8). Tumor lesions were analyzed 14 weeks after injection. Bars = 100 µm. (B) Box plot showing tumor burden in each affected mammary gland of *Cdh1*$^{F/F}$;*Pten*$^{F/F}$ mice injected with Lenti-Cre. (C) Representative immunofluorescence imaging of tumor sections from Lenti-Cre injected *Cdh1*$^{F/F}$;*Pten*$^{F/F}$ mice, stained with antibodies against CK8, PTEN and E-cadherin. Bar = 25 µm. (D) Recombination status of *Cdh1* and *Pten* alleles in Lenti-Cre induced *Cdh1*$^{F/F}$;*Pten*$^{F/F}$ tumors, as visualized by PCR. EcadF/PtenF and EcadD/PtenD are PCRs to detect the *Cdh1*^{F}/*Pten*^{F} or *Cdh1*$^{\Delta}$/*Pten*$^{\Delta}$ alleles, respectively.

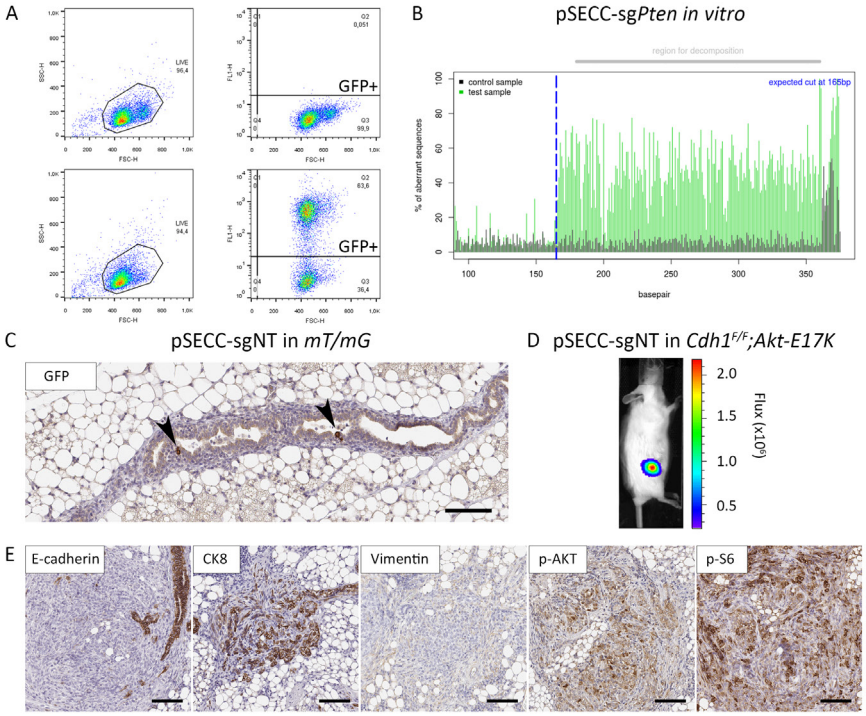

Supplementary Figure S5

pSECC vector performance *in vitro* and *in vivo*. (A) FACS analysis of GFP expression in pSECC-sg*Pten*-transduced Cre-reporter cells 5 days after transduction. (B) TIDE analysis of the targeted *Pten* alleles in pSECC-sg*Pten*-transduced Cre-reporter cells, showing nucleotide signal of gene-edited (green) and control (black) populations. The blue dotted line indicates the expected cutting site. The gray horizontal bar above the graph shows the region used for TIDE decomposition. (C) Immunohistochemical detection of GFP expression in a mammary gland section from *mT/mG* Cre-reporter mice intraductally injected with pSECC-sgNT (n=8). Arrowheads indicate GFP positive cells. Mice were analyzed 14 days after injection. Bar = 100 µm. (D) Representative *in vivo* bioluminescence imaging of luciferase expression in a pSECC-sgNT injected *Cdh1*$^{F/F}$*;Akt-E17K* mouse 16 weeks after injection. (E) Immunohistochemical analysis of E-cadherin, CK8, vimentin, phospho-AKT^{Ser473}, and phospho-S6 $^{Ser235/236}$ expression in tumor sections from *Cdh1*$^{F/F}$*;Akt-E17K* mice injected with pSECC-sgNT (n=4). Tumor lesions were analyzed 16 weeks after injection. Bars = 100 µm.

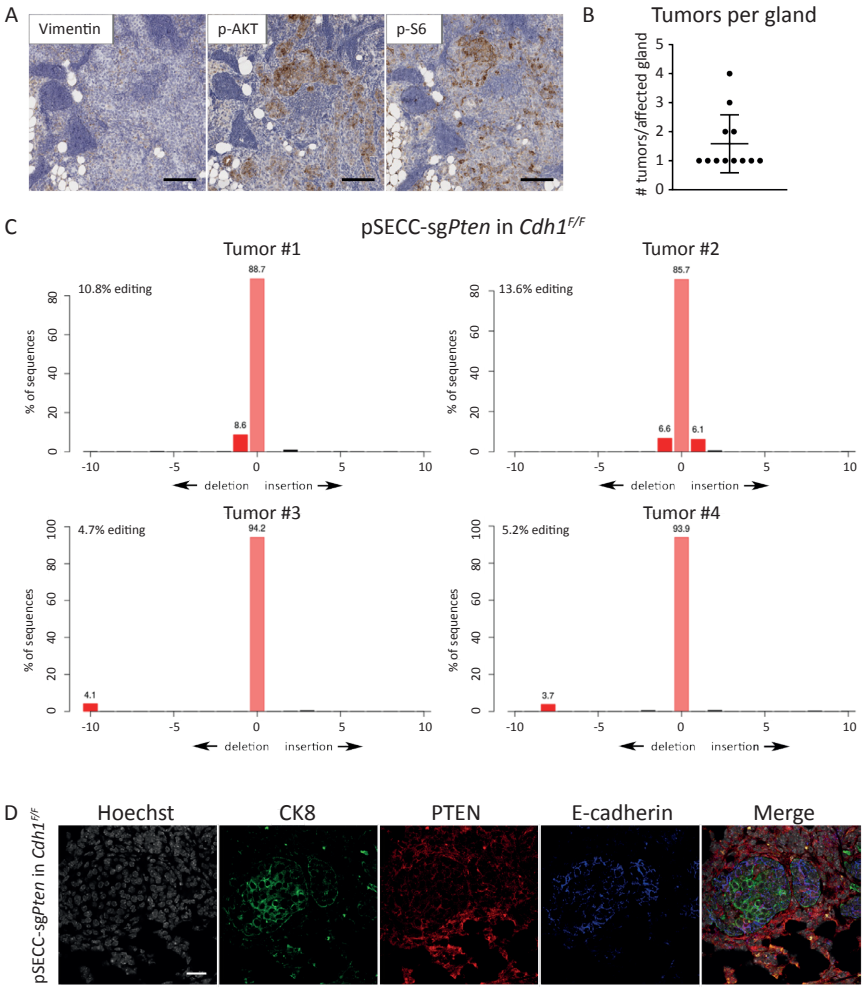

Supplementary Figure S6

Analysis of mammary gland tumors in *Cdh1*$^{F/F}$ mice injected with pSECC-sg*Pten*. (A) Immunohistochemical analysis of vimentin, phospho-AKT^{Ser473}, and phospho-S6$^{Ser235/236}$ expression in tumor sections from *Cdh1*$^{F/F}$ mice injected with pSECC-sg*Pten*. Tumors were analyzed 25 weeks after injection. Bars = 100 µm. (B) Box plot showing number of tumors detected in each affected mammary gland of *Cdh1*$^{F/F}$ mice injected with pSECC-sg*Pten* (n=48). (C) TIDE analysis of the targeted *Pten* alleles in independent tumor lesions from pSECC-sg*Pten* injected *Cdh1*$^{F/F}$ mice, showing positive selection for frame-shifting indels. (D) Representative immunofluorescence imaging of tumor sections from pSECC-sg*Pten* injected *Cdh1*$^{F/F}$ mice, stained with antibodies against CK8, PTEN and E-cadherin. Bar = 25 µm.

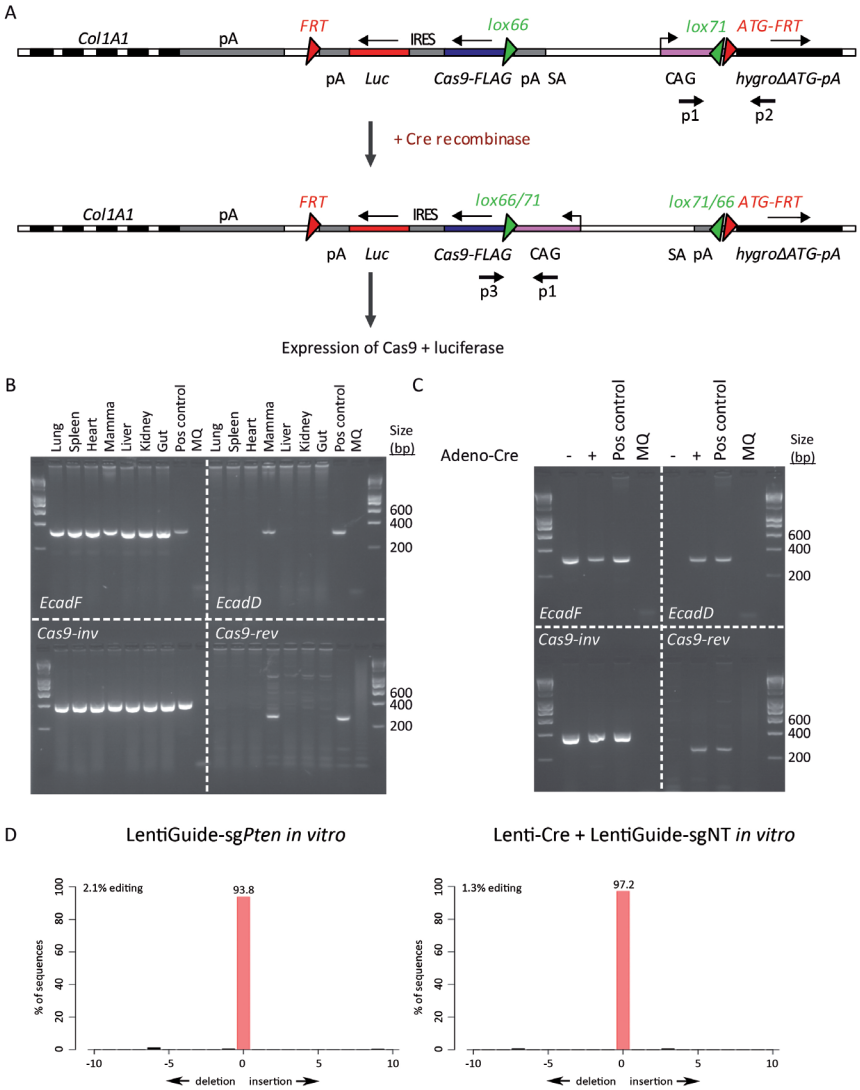

Supplementary Figure S7

Schematic overview of the conditional Cas9 knock-in allele. (A) Depiction of the Cre-conditional *invCAG-Cas9-IRES-Luc* allele integrated into the *Col1a1* locus of embryonic stem cells (ESCs) derived from *WapCre;Cdh1*$^{F/F}$ mice. WapCre-mediated recombination allows mammary-specific inversion of CAG promoter, resulting in expression of Cas9 and luciferase. (B) Recombination status of the Cre-conditional *Cas9* allele and *Cdh1* alleles in different organs isolated from 12-weeks old *WapCre;Cdh1*$^{F/F}$*;Cas9* females, as visualized by PCR. EcadF and EcadD are PCRs to detect the *Cdh1*^{F} or *Cdh1*^{Δ} alleles, respectively. Cas9-inv and Cas9-rev are PCRs to detect the inactive or active orientation of the Cre-conditional Cas9 allele, respectively. Primer positions are shown in panel A. (C) Recombination of the Cre-conditional *Cas9* allele and *Cdh1* alleles following *in vitro* transduction of *Cdh1*$^{F/F}$*;Cas9* MMECs with Adeno-Cre, as visualized by PCR. (D) TIDE analysis of the targeted *Pten* alleles in control *Cdh1*$^{F/F}$*;Cas9* MMECs transduced with LentiGuide-sg*Pten* or co-transduced with Lenti-Cre and LentiGuide-sgNT. Cells were analyzed 5 days after transduction.

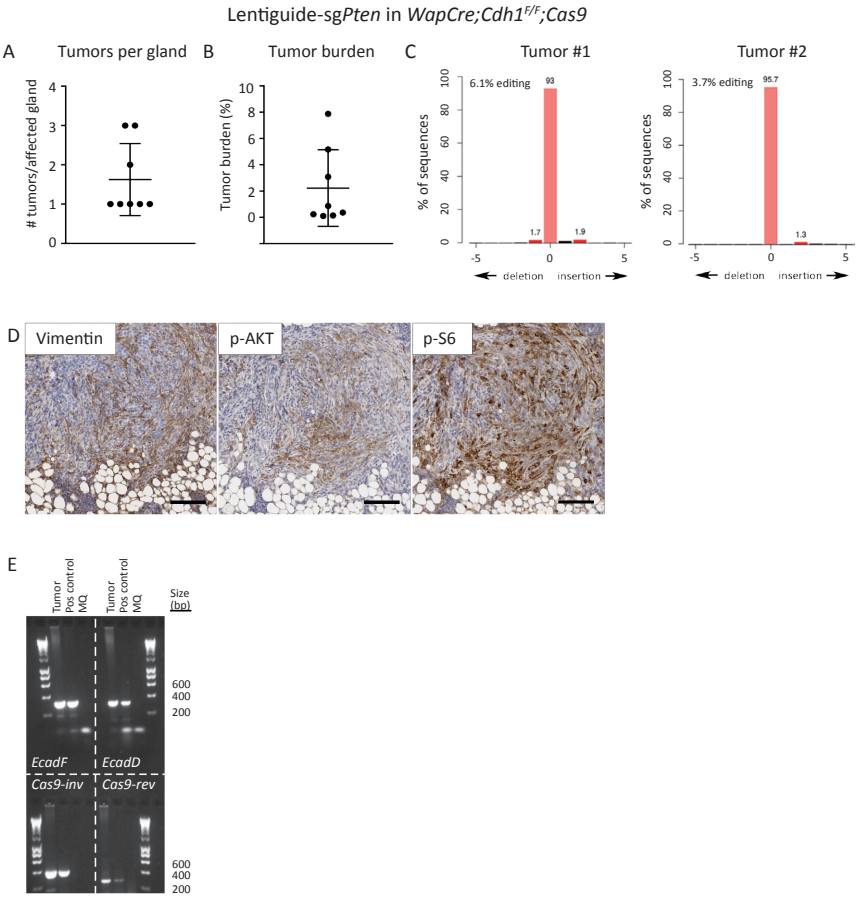

Supplementary Figure S8

Analysis of mammary tumors in *WapCre;Cdh1*$^{F/F}$*;Cas9* mice injected with LentiGuide-sg*Pten*. (A) Box plot showing number of tumors detected in each affected mammary gland of *WapCre;Cdh1*$^{F/F}$*;Cas9* mice injected with LentiGuide-sg*Pten* (n=27). Mammary glands were harvested and analyzed 25 weeks after injection. (B) Box plot showing tumor burden in each affected mammary gland of *WapCre;Cdh1*$^{F/F}$*;Cas9* mice injected with LentiGuide-sg*Pten*. (C) TIDE analysis of the targeted *Pten* alleles in independent lesions from *WapCre;Cdh1*$^{F/F}$*;Cas9* mice injected with LentiGuide-sg*Pten*, showing positive selection for frame-shifting indels. (D) Immunohistochemical analysis of vimentin, phospho-AKT^{Ser473}, and phospho-S6$^{Ser235/236}$ expression in tumor sections from *WapCre;Cdh1*$^{F/F}$*;Cas9* mice injected with LentiGuide-sg*Pten*. Bars = 100 µm. (E) Recombination status of the Cre-conditional *Cas9* allele and *Cdh1* alleles in a LentiGuide-sg*Pten* induced *WapCre;Cdh1*$^{F/F}$*;Cas9* tumor, as visualized by PCR.

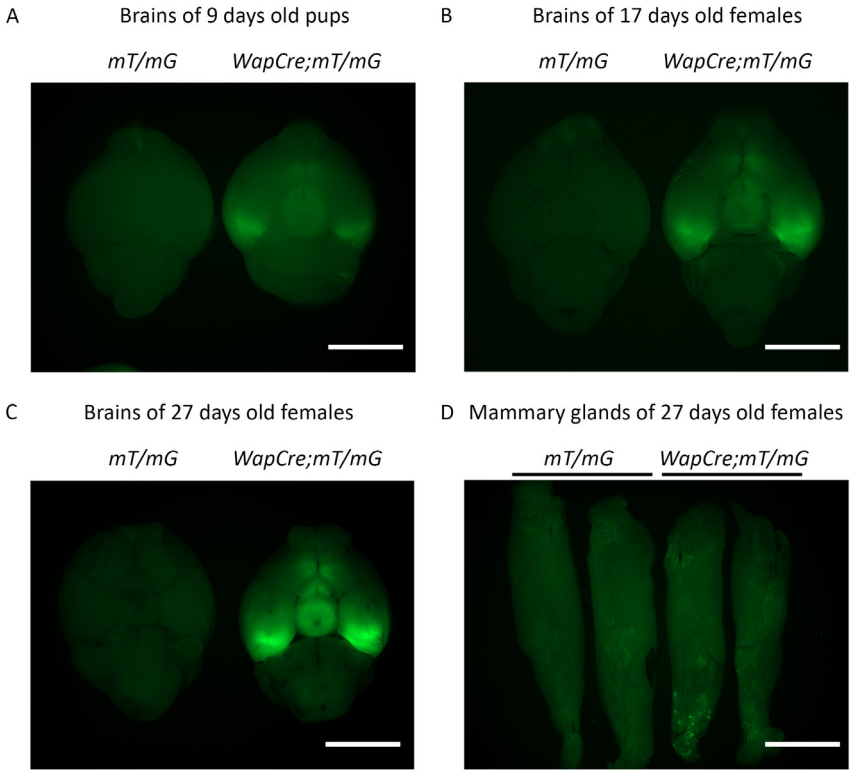

Supplementary Figure S9

WapCre expression in pre-puberal *mT/mG* Cre-reporter mice. (A-C) Fluorescence microscopy of GFP expression in the ventral brain from *WapCre;mT/mG* mice at different stages of postnatal development, showing GFP expression building up over time in the piriform cortex (n=6). Bars = 5 mm. (D) Fluorescence microscopy of GFP expression in mammary glands from 27-days old *WapCre;mT/mG* females (n=3). Bar = 5 mm.

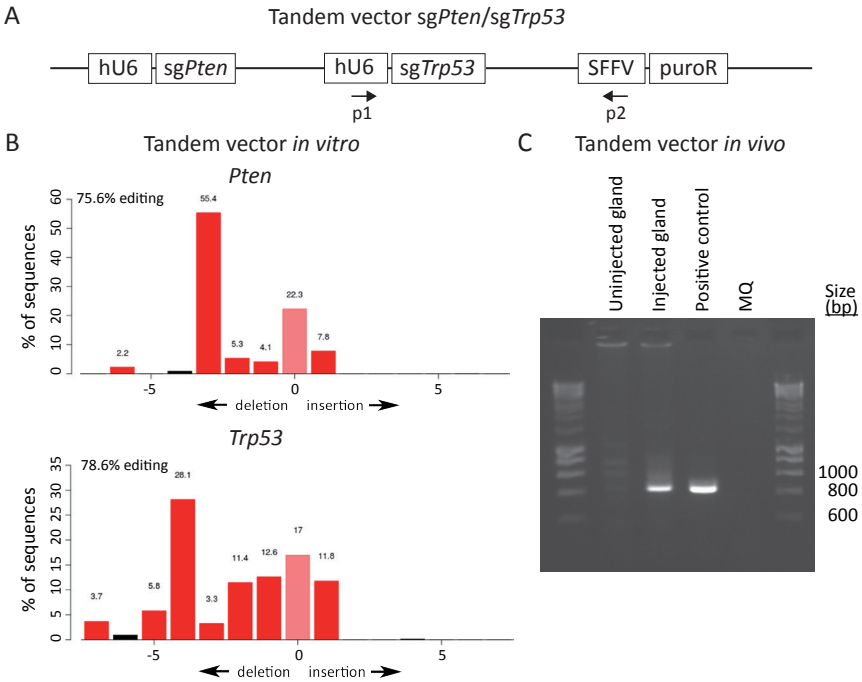

Supplementary Figure S10

Intraductal injection of tandem sgRNA vectors. (A) Schematic overview of the tandem sgRNA vector encoding sg*Pten* and sg*Trp53* (sg*Pten*/sg*Trp53*). hU6, human U6 promoter; SFFV, Spleen Focus-Forming Virus promoter; puroR, puromycin resistance gene. (B) TIDE analysis of the targeted *Pten* and *Trp53* alleles in Cas9-expressing cells transduced with the tandem sg*Pten*/sg*Trp53* vector reveals specific indels at both loci. Cells were analyzed 5 days after transduction. As a control, cells transduced with a sgNT/sgNT tandem vector were used. (C) Detection of the integrated tandem sg*Pten*/sg*Trp53* vector in mammary glands of *WapCre;Cdh1*$^{F/F}$*;Cas9* mice injected with sg*Pten*/sg*Trp53*, as visualized by PCR. Mammary epithelial cells were isolated and analyzed 2 weeks post-injection. Primer positions are shown in panel A.